Ab responses for mice given rPspA plus pFL were comparable to those seen for mice given nasal nCT vaccination (Fig. 3A). To further support these findings, elevated numbers of PspA-specific IgA AFCs were detected in NPs, CLNs, NALT, lungs, and MeLNs of mice given nasal rPspA and pFL (Fig. 3B). In addition, significantly higher numbers of rPspA-specific IgG and/or IgM AFCs were seen for mice given pFL as a nasal adjuvant than for mice given nasal pORF or rPspA alone (Fig. 3B). These results clearly show that pFL as a nasal adjuvant effectively elicits rPsp-specific Ab responses in mucosa-associated lymphoid tissues in the respiratory tract. Since nasal immunization is known to induce systemic immunity in addition to the mucosa, rPspA-specific Ab responses in plasma and spleen were examined. Nasal pFL as a mucosal adjuvant successfully enhanced rPspA-specific IgG and IgA Ab responses in plasma which are comparable to those responses seen in mice given nasal rPspA plus nCT (Fig. 4A). Thus, significantly increased numbers of rPspA-specific IgM, IgG, and IgA AFCs were seen in spleen of mice given pFL as a nasal adjuvant (Fig. 4B). When the levels of rPspA-specific IgG subclass Ab responses were examined, increased levels of anti-rPspA IgG1, IgG2a, and IgG2b Abs were noted for mice given nasal rPspA plus pFL compared with those Ab responses for mice given rPspA plus pORF or rPspA alone (Fig. 4A). Essentially no IgG3 Ab response against rPspA was detected. Taken together, pFL as a nasal adjuvant effectively induces rPspA-specific Ab responses in both mucosal and systemic immune compartments.

Nasal rPspA plus pFL leads CD11b$^+$ and CD8$^+$ DCs. Since our previous studies reported that nasal pFL plus ovalbumin as an Ag elicited expansion of CD8-expressing lymphoid-type CD11c$^+$ DCs (19), we next characterized CD11c$^+$ DCs in the various mucosal tissues of mice given rPspA plus pFL or pORF. Nasal immunization of rPspA plus pFL significantly increased the frequency of CD11c$^+$ cells in both mucosal and systemic tissues compared with results for mice given rPspA plus pORF (Table 1). Interestingly, the numbers of CD8$^+$ DCs were increased in all tissues of mice given pFL as a nasal adjuvant compared with those numbers for mice given nasal pORF. In addition, increased frequencies of CD11b$^+$ DCs were noted in NALT, NPs, CLNs, and spleen. In contrast, increased frequencies of B220$^+$ DCs were seen only in CLNs (Table 1). Further, higher expression of major histocompatibility complex class II (MHC II), CD40, CD80, and CD86 was seen on CD11c$^+$ DCs (Table 1). CD8$^+$ and CD11b$^+$ DCs from NALT, lungs, and NPs were also examined by fluorescence-activated cell sorting (FACS) for expression of costimulatory molecules. Our results showed increased frequencies of costimulatory molecule expression by CD8$^+$ and CD11b$^+$ DCs in the tissues of mice given nasal pFL compared with those in control groups (Table 2). Taken together, these results indicate that nasal administration of rPspA plus pFL preferentially expands the numbers of CD8$^+$ and CD11b$^+$ DC populations which express elevated levels of costimulatory molecules.

Th1- and Th2-type cytokine responses by PspA-specific CD4$^+$ T cells. We next assessed rPspA-specific CD4$^+$ T cell responses induced by pFL as a mucosal adjuvant. rPspA-stimulated CD4$^+$ T cells from lungs, CLNs, and spleen of mice given nasal rPspA plus pFL showed significantly higher proliferative responses than did those from mice nasally immunized

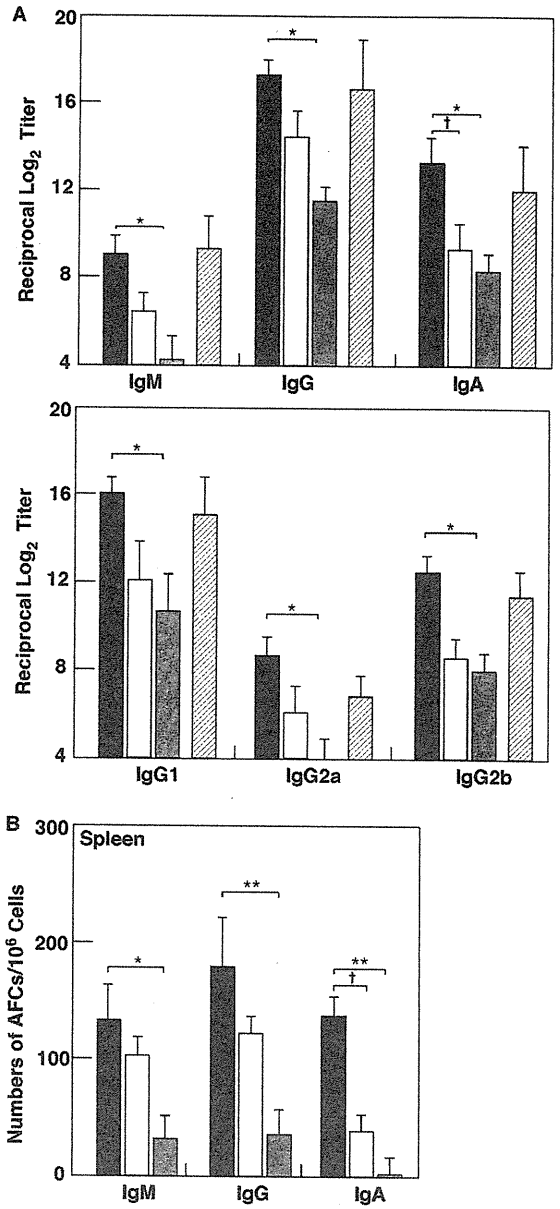

FIG. 4. Comparison of rPspA-specific Ab responses in plasma and spleen cells of mice given nasal rPspA plus pFL (black column) or pORF (white column), rPspA alone (shaded column), or rPspA plus nCT (hatched column). Each mouse group was nasally immunized weekly for three consecutive weeks. (A) Seven days after the last immunization, rPspA-specific IgM, IgG, IgA, and IgG subclass Ab responses in plasma were determined by Ag-specific ELISA. An rPspA-specific IgG3 Ab response was not detected. (B) Seven days after the last immunization, mononuclear cells were isolated from spleens and were then subjected to ELISPOT assay to determine numbers of rPspA-specific IgM, IgG, and IgA AFCs. The values shown are the means ± SEM (n = 20). *, $P < 0.05$; **, $P < 0.01$ (compared with results for mouse group given rPspA alone). †, $P < 0.05$ (compared with results for mouse group given rPspA plus pORF).

with rPspA plus pORF (Table 3). In this regard, when Th1- and Th2-type cytokine profiles were examined, PspA-stimulated CD4$^+$ T cells from mice given pFL as a nasal adjuvant exhibited higher levels of IL-2, IL-4, IL-5, and IL-6 production than those in control mice. On the other hand, levels of IFN-γ

TABLE 1. Frequencies of CD11c$^+$ DCs and CD8, CD11b, B220, and costimulatory molecule expression by CD11c$^+$ DCs of mucosal effector and inductive tissues of mice given nasal rPspA with pFL or pORF[a,e]

Tissue source	Adjuvant given with nasal rPspA	% CD11c$^+$ total lymphocytes[b]	% CD11c$^+$ DCs expressing:						
			CD8[c]	CD11b[c]	B220[c]	CD40[d]	CD80[d]	CD86[d]	MHC II[d]
NALT	pFL	*6.6 ± 1.7	*23.5 ± 3.7	*23.1 ± 3.1	56.5 ± 6.2	**3.1 ± 0.7	10.9 ± 4.5	*19.3 ± 4.8	**68.9 ± 8.2
	pORF	1.7 ± 1.2	12.1 ± 1.6	12.3 ± 3.9	50.4 ± 0.6	0.4 ± 0.5	5.9 ± 1.6	8.9 ± 2.6	45.9 ± 1.9
Lungs	pFL	*5.7 ± 1.3	*12.4 ± 2.4	68.6 ± 4.1	24.8 ± 3.5	*4.6 ± 1.1	*15.2 ± 5.6	*20.8 ± 3.6	*51.5 ± 9.6
	pORF	3.3 ± 1.6	7.7 ± 0.9	63.9 ± 3.9	20.6 ± 4.7	1.6 ± 0.1	6.9 ± 2.4	9.5 ± 7.9	39.1 ± 0.7
NPs	pFL	*10.1 ± 2.4	*22.1 ± 2.3	*60.1 ± 6.9	19.3 ± 3.7	*11.1 ± 3.3	*23.8 ± 3.5	25.9 ± 6.2	38.5 ± 4.2
	pORF	5.3 ± 0.9	14.8 ± 3.8	31.1 ± 6.0	20.6 ± 4.7	3.6 ± 0.7	17.8 ± 0.1	23.1 ± 7.6	33.3 ± 1.9
CLNs	pFL	*2.3 ± 0.4	*32.8 ± 3.6	*31.8 ± 3.6	*45.4 ± 4.1	**3.1 ± 0.2	**24.7 ± 1.0	*43.3 ± 2.9	87.4 ± 5.9
	pORF	0.7 ± 0.2	21.1 ± 3.6	24.8 ± 3.2	33.3 ± 4.5	0.7 ± 0.9	10.6 ± 1.3	28.5 ± 8.5	85.3 ± 0.6
Spleen	pFL	*2.4 ± 0.7	*21.7 ± 2.2	*33.4 ± 5.1	44.6 ± 3.5	*4.3 ± 2.0	20.3 ± 6.4	**26.4 ± 5.3	**87.5 ± 1.5
	pORF	1.4 ± 0.5	18.2 ± 0.9	25.2 ± 3.4	39.9 ± 3.5	1.1 ± 0.1	12.9 ± 0.6	11.4 ± 2.8	75.0 ± 4.2

[a] Mononuclear cells from NALT, lungs, NPs, CLNs, and spleens of mice immunized with rPspA plus pFL or pORF were stained with a combination of anti-CD11c and the respective MAb and subjected to FACSCalibur flow cytometry analysis.
[b] Mononuclear cells were stained with PE-conjugated anti-CD11c MAb and subjected to flow cytometry analysis.
[c] Mononuclear cells were stained with FITC-conjugated anti-CD8α, -CD11b, and -B220 MAb and PE-labeled anti-CD11c.
[d] Mononuclear cells were stained with PE-labeled anti-CD40, -CD80, -CD86 or I-A^b and biotinylated anti-mouse CD11c MAb followed by CyChrome-streptavidin.
[e] *, $P < 0.05$; **, $P < 0.01$ (compared with those of mice immunized with rPspA plus pORF).

production by PspA-stimulated CD4$^+$ T cells were essentially the same between mice given pFL or pORF (Table 3). Intracellular IL-17 analysis revealed that no significant increase in the frequency of IL-17-producing CD4$^+$ T cells was seen in CLNs and spleen of mice given nasal pFL compared with results for mice given empty plasmid as a nasal adjuvant (data not shown). These results show that pFL as a nasal adjuvant preferentially induces Th2-type dominant cytokine responses in the lower respiratory mucosa when rPspA is used as an Ag for nasal vaccination.

Protection against *S. pneumoniae* infection by nasal vaccination with rPspA plus pFL. In order to determine the functional properties of nasal vaccination with rPspA plus pFL, mice were challenged with *S. pneumoniae* strain WU2 (1.8×10^7 CFU/20 μl) 1 week after the last vaccination. When the bacterial densities in the lungs, NWs, and blood were examined 48 h after nasal challenge, mice given nasal rPspA plus pFL showed significantly lower bacterial density. Conversely, lungs, NWs, and blood of mice given rPspA plus pORF contained high numbers of *S. pneumoniae* bacteria (Fig. 5). These results show that nasal rPspA plus pFL provides effective protection against *S. pneumoniae* infection at the lung and nasal mucosa.

DISCUSSION

In this study, we have investigated whether nasal pFL as a mucosal adjuvant elicits functional bacterial Ag (rPspA)-specific Ab responses for protection against *S. pneumoniae* infection. Our results clearly showed that nasal vaccination with rPspA plus pFL elicited DC-mediated Th2-type and IL-2 cytokine responses and subsequent anti-rPspA Abs for protection against pneumococcal infection at the pulmonary mucosa. Since a risk of central nervous system toxicity is one of the major issues for nasal vaccine development (6, 9, 29), we also examined pFL uptake and inflammatory cytokine synthesis in the nasal mucosa. Our results indicated that nasal pFL was taken up only by NALT and NP DCs, as well

TABLE 2. Frequencies of costimulatory molecule expression on CD8 or CD11b DCs in mucosal effector and inductive tissues of mice given nasal rPspA with pFL or pORF[a]

Tissue source	Adjuvant given with nasal rPspA	% CD11c$^+$ DCs							
		CD8$^+$ DCs				CD11b$^+$ DCs			
		CD40	CD80	CD86	MHC II	CD40	CD80	CD86	MHC II
NALT	pFL	**1.4 ± 0.1	*4.4 ± 0.6	*9.5 ± 1.4	**34.5 ± 2.2	**1.3 ± 0.1	*4.1 ± 0.3	*8.5 ± 1.7	*27.3 ± 4.2
	pORF	0.2 ± 0.1	2.0 ± 0.4	4.0 ± 0.7	12.4 ± 1.3	0.2 ± 0.1	1.7 ± 0.2	3.7 ± 1.0	14.6 ± 1.5
Lungs	pFL	*1.7 ± 0.2	**7.7 ± 0.3	**7.5 ± 0.4	**18.7 ± 3.1	*1.4 ± 0.2	*6.6 ± 0.9	*8.0 ± 0.8	*30.5 ± 3.8
	pORF	0.5 ± 0.1	1.3 ± 0.1	2.3 ± 0.2	6.2 ± 1.0	0.9 ± 0.3	3.5 ± 0.9	3.6 ± 1.0	14.5 ± 5.7
NPs	pFL	*5.8 ± 0.4	*8.2 ± 1.7	*9.8 ± 1.5	*14.8 ± 2.4	*4.5 ± 1.1	*13.1 ± 2.0	11.5 ± 3.3	*20.6 ± 3.5
	pORF	1.4 ± 0.3	4.9 ± 1.4	4.9 ± 1.0	7.3 ± 1.9	2.5 ± 1.0	7.0 ± 1.7	8.7 ± 2.0	12.0 ± 2.2

[a] CD11c-positive DCs from NALT, lungs, and NPs of mice immunized with rPspA plus pFL or pORF were purified from mononuclear cells by using the automatic cell sorter system AutoMacs and were stained with a combination of FITC-conjugated anti-mouse CD8α MAb or anti-mouse CD11b MAb and PE-labeled anti-CD40, -CD80, -CD86, or I-A^b and subjected to FACSCalibur flow cytometry analysis. *, $P < 0.05$; **, $P < 0.01$ (compared with those of mice immunized with rPspA plus pORF).

TABLE 3. $CD4^+$ Th1- and Th2-type cytokine responses after *in vitro* restimulation with rPspA[a]

Tissue	Nasal adjuvant	Stimulation index[b]	Production of Th1- or Th2-type cytokine[c]					
			IFN-γ (ng/ml)	IL-2 (pg/ml)	IL-4 (pg/ml)	IL-5 (pg/ml)	IL-6 (ng/ml)	IL-10 (ng/ml)
Lungs	pFL	*5.5 ± 1.8	2.03 ± 0.40	*249.8 ± 48.8	*56.7 ± 9.4	*255.7 ± 76.9	*1.80 ± 0.49	1.19 ± 0.32
	pORF	2.5 ± 0.6	1.48 ± 0.24	130.1 ± 35.7	21.2 ± 4.4	86.6 ± 22.0	0.78 ± 0.29	0.89 ± 0.34
CLNs	pFL	*6.1 ± 1.3	1.63 ± 0.24	*201.3 ± 55.3	*55.6 ± 14.9	*314.5 ± 66.6	1.51 ± 0.68	1.43 ± 0.41
	pORF	2.4 ± 0.2	1.13 ± 0.18	78.8 ± 13.6	18.8 ± 5.40	66.5 ± 28.8	0.72 ± 0.34	1.21 ± 0.47
Spleen	pFL	*4.8 ± 1.4	1.65 ± 0.47	*391.1 ± 68.9	*45.1 ± 10.5	*286.8 ± 53.4	*1.33 ± 0.50	1.57 ± 0.39
	pORF	1.9 ± 0.4	1.22 ± 0.39	53.3 ± 19.1	16.1 ± 6.20	57.7 ± 15.1	0.89 ± 0.42	1.40 ± 0.24

[a] The $CD4^+$ T cells (4×10^6 cells/ml) from lungs, CLNs, and spleen were isolated 7 days after the last immunization with rPspA (5 μg) and pFL or pORF as a mucosal adjuvant and cultured with T cell depleted feeder cells (8×10^6 cells/ml). Values are presented as means ± SEM of data from 30 mice for each group and a total of three experiments. *, $P < 0.05$ when compared with mice given rPspA plus pORF.

[b] Proliferative responses of $CD4^+$ T cells from mice nasally immunized with rPspA plus pFL or pORF as a mucosal adjuvant were represented as the stimulation index by measuring counts per minute (cpm) of wells with or without rPspA (control). The levels of [^{3}H]TdR incorporation for each control well were between 500 and 1,000 cpm. The results show the individual values from these separate experiments of 30 mice per experimental group.

[c] The culture supernatant were harvested after 48 h of incubation and subjected to the respective cytokine ELISAs.

as nECs, but not by ON/E. Further, minimal levels of IL-1β, IL-6, and TNF-α production were induced in NWs of mice given pFL. Taken together, the current study is the first to show that nasal pFL is a safe mucosal adjuvant that effectively elicits bacterial Ag (PspA)-specific functional Ab responses that are potent for the prevention of pneumococcal pneumonia and bacteremia.

We recently showed that pFL as a nasal adjuvant elicited PspA-specific S-IgA Ab responses in the nasal cavity to prevent nasal carriage of *S. pneumoniae* (12). Although the recent study clearly indicated the potential of pFL as a nasal adjuvant for a pneumococcal vaccine, it still remained to be elucidated whether pFL can induce protection in the lower respiratory mucosa, including the lungs. In this regard, nasal pFL elicited functional rPspA-specific S-IgA Ab responses in the BALF and lungs when mice given nasal rPspA plus pFL were nasally challenged with a large amount (20 μl; 1.8×10^7 CFU) of WU2 (invasive strain), allowing bacterial exposure to the lungs. Thus, mice given nasal rPspA plus pFL showed a significantly lower number of bacteria in the BALF after being challenged fatally with WU2 than did mice given empty plasmid as a nasal adjuvant. Based upon our previous studies and those of others (12, 42), we expected that nasal immunization with rPspA plus pFL induced Ag-specific functional S-IgA Ab responses in the nasal cavity. Indeed, a remarkable anti-rPspA S-IgA Ab induction and the inhibition of bacterial growth were seen in NWs after bacterial challenge. Thus, it is possible that an effective inhibition of nasopharyngeal bacterial colonization might lead to drastic reduction of bacterial growth in the lungs and prevention of subsequent bacteremia. In any case, the presence of anti-PspA IgA Abs in the lower and upper respiratory mucosa is the fundamental factor to prevent bacterial invasion of the hosts.

The FL protein is known as a synergistic hematopoietic growth factor that has emerged as a potential immunomodulator (8, 21, 38) and can expand DC populations and enhance antigen-presenting cell (APC) activity (13, 24). In

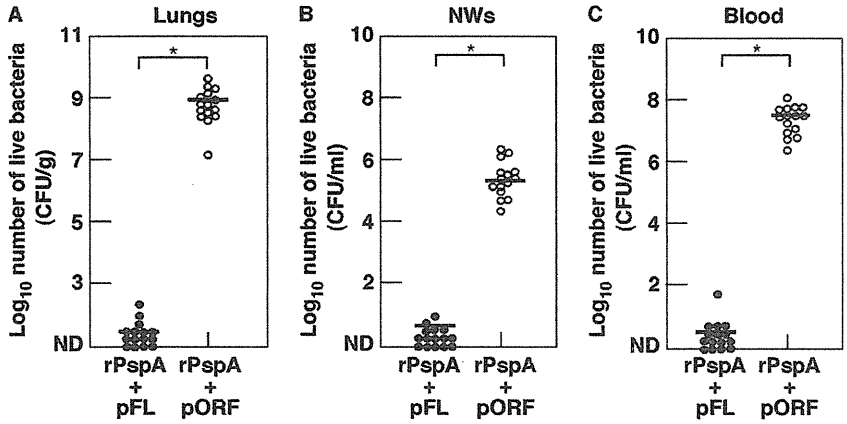

FIG. 5. Comparison of protective effects against *S. pneumoniae* infection with nasal pFL-based rPspA vaccine. One week after the last immunization with rPspA plus pFL (closed circle) or pORF (open circle), mice were challenged with 1.8×10^7 CFU of the WU2 strain. (A) Forty-eight hours after bacterial challenge, the lungs were removed aseptically and homogenized in 9 ml of sterile saline per gram of lung tissue for the culture. (B) NWs were harvested aseptically by flushing with 1 ml of PBS and cultured on agar medium. (C) Blood samples were plated on agar medium from the culture. The detection limit of bacterial cultures was 10^2 CFU/g. The values shown are the means ± SEM ($n = 15$). Each line represents the median $\log_{10}$ CFU/mouse. *, $P < 0.05$, compared with mouse group given rPspA plus pORF.

addition, it was recently reported that percutaneous administration of the FL protein regulated migration and Ag uptake of lung DCs (34, 35). In this regard, our previous studies showed that nasal pFL increases the frequency of $CD8^+$ DCs in various mucosal and systemic lymphoid tissues (11, 19). Our present study showed increased numbers of $CD8^+$ DCs, which agrees with these previous findings even though a bacterial Ag was used as a component of the nasal vaccine. Since a recent study indicated that induction of $CD8^+$ DCs promoted protection against respiratory infection (7), it is possible that induction of $CD8^+$ DCs in the mucosal and systemic compartments contributes to *S. pneumoniae* clearance in the respiratory tract and blood. Further, increased frequencies of $CD11b^+$ DCs were also seen in mice given nasal rPspA plus pFL. Recent reports showed that the interactions between $CD4^+$ T cells and DCs play a key role in the induction of pulmonary immunity (1) and that DCs polarize initial $CD4^+$ T cell activation toward Th2-type immune responses (33). Further, our previous and present studies showed that nasal pFL elicited $CD8^+$ DC-mediated Th2-type responses. In this regard, it is possible that $CD11b^+$ DCs play a role in the downregulation of Th2-prone cytokine responses for the maintenance of mucosal homeostasis. Indeed, it was suggested that FL treatment induced Th2-suppressive lung $CD11b^+$ DCs (15, 35). Further, nasal application of FL-expressing adenovirus as a mucosal adjuvant preferentially expands $CD11b^+$ DCs to produce a balanced Th1- and Th2-type cytokine response (32). The actual immunoregulatory functions of $CD11b^+$ DCs induced by nasal pFL are currently being tested in our laboratory.

In summary, the present study shows that pFL as a nasal adjuvant induces enhanced PspA-specific immunity in the nasal-pulmonary mucosa via $CD8^+$ and $CD11b^+$ DC subset-mediated Th2-type cytokines responses. Importantly, nasal vaccination with rPspA plus pFL inhibits bacterial growth in the lungs and nasal cavities of mice in order to prevent the early phases of pneumococcal pneumonia without CNS toxicity or inflammation. These findings suggest that pFL is a safe nasal adjuvant for use in the future development of vaccines that can induce enhanced specific immunity against bacterial and viral Ags.

ACKNOWLEDGMENTS

We are grateful to Jerry R. McGhee and Rebekah S. Gilbert for scientific discussion, critiques, and editorial assistance in the preparation of the manuscript.

This work is supported by NIH grants AG 025873 and DE 012242 and a Grant-in Aid for Challenging Exploratory Research (22659383) and grant B-23390481 from the Japan Society for the Promotion of Science and Scholarship of the Fujii-Otsuka Foundation for International Research, as well as the Biomedical Cluster Kansai project, which is promoted by the Regional Innovation Cluster Program, subsidized by the Japanese Government and the Program for Promotion of Fundamental Studies in Health Sciences of the National Institute of Biomedical Innovation (NIBIO).

REFERENCES

1. **Bakocevic, N., T. Worbs, A. Davalos-Misslitz, and R. Forster.** 2010. T cell-dendritic cell interaction dynamics during the induction of respiratory tolerance and immunity. J. Immunol. **184:**1317–1327.
2. **Bogaert, D., R. de Groot, and P. W. M. Hermans.** 2004. *Streptococcus pneumoniae* colonization: the key to pneumococcal disease. Lancet Infect. Dis. **4:**144–154.
3. **Briles, D. E., et al.** 2000. Intranasal immunization of mice with a mixture of the pneumococcal proteins PsaA and PspA is highly protective adjuvant nasopharyngeal carriage of *Streptococcus pneumoniae*. Infect. Immun. **68:** 796–800.
4. **Briles, D. E., et al.** 2000. Immunization of human recombinant pneumococcal surface protein A (rPspA) elicits antibodies that passively protect mice from fatal infection with *Streptococcus pneumoniae* bearing heterologous PspA. J. Infect. Dis. **182:**1694–1701.
5. **Briles, D. E., et al.** 1996. Systemic and mucosal protective immunity to pneumococcal surface protein A. Ann. N. Y. Acad. Sci. **797:**118–126.
6. **Couch, R. B.** 2004. Nasal vaccination, Escherichia coli enterotoxin, and Bell's palsy. N. Engl. J. Med. **350:**860–861.
7. **Dunne, P. J., B. Moran, R. C. Cummins, and K. H. G. Mills.** 2009. $CD11c^+$ $CD8^+$ dendritic cells promote protective immunity to respiratory infection with *Bordetella pertussis*. J. Immunol. **183:**400–410.
8. **Edwan, J. H., G. Perry, J. E. Talmadge, and D. K. Agrawal.** 2004. Flt-3 ligand reverses late allergic response and airway hyper-responsiveness in a mouse model of allergic inflammation. J. Immunol. **172:**5016–5023.
9. **Fujihashi, K., T. Koga, F. van Ginkel, Y. Hagiwara, and J. R. McGhee.** 2002. A dilemma for mucosal vaccination: efficacy versus toxicity using enterotoxin-based adjuvants. Vaccine **20:**2431–2438.
10. **Fujihashi, K., et al.** 1996. gamma/delta T cell-deficient mice have impaired mucosal IgA responses. J. Exp. Med. **183:**1929–1935.
11. **Fukuiwa, T., et al.** 2008. A recombination of Flt3 ligand cDNA and CpG ODN as nasal adjuvant elicits NALT dendritic cells for prolonged mucosal immunity. Vaccine **26:**4849–4859.
12. **Fukuyama, Y., et al.** 2010. Secretory-IgA antibodies play an important role in the immunity to *Streptococcus pneumoniae*. J. Immunol. **185:**1755–1762.
13. **Gilliland, D. G., and J. D. Griffin.** 2002. The roles of FLT3 in hematopoiesis and leukemia. Blood **100:**1532–1542.
14. **Hagiwara, H., et al.** 2006. A second generation of double mutant cholera toxin adjuvants: enhanced immunity without intracellular trafficking. J. Immunol. **177:**3045–3054.
15. **Hammad, H., et al.** 2004. Differential capacity of $CD8a^+$ or $CD8a^-$ dendritic cell subsets to prime for eosinophilic airway inflammation in the T-helper type 2-prone milieu of the lung. Clin. Exp. Allergy **34:**1834–1840.
16. **Imaoka, K., et al.** 1998. Nasal immunization of nonhuman primates with simian immunodeficiency virus p55 gag and cholera toxin adjuvant induces Th1/Th2 help for virus-specific immune responses in reproductive tissues. J. Immunol. **161:**5952–5958.
17. **Kataoka, K., and K. Fujihashi.** 2009. Dendritic cell-targeting DNA-based mucosal adjuvants for the development of mucosal vaccines. Expert Rev. Vaccines **8:**1183–1193.
18. **Kataoka, K., et al.** 2007. Nasal cholera toxin elicits IL-5 and IL-5 receptor a-chain expressing B-1a B cells for innate mucosal IgA antibody responses. J. Immunol. **178:**6058–6065.
19. **Kataoka, K., et al.** 2004. Nasal Flt3 ligand cDNA elicits $CD11c^+$ $CD8^+$ dendritic cells for enhanced mucosal immunity. J. Immunol. **172:**3612–3619.
20. **Kurono, Y., et al.** 1999. Nasal immunization induces *Haemophilus influenzae*-specific Th1 and Th2 responses with mucosal IgA and systemic IgG antibodies for protective immunity. J. Infect. Dis. **180:**122–132.
21. **Kutzler, M. A., and D. B. Weiner.** 2004. Developing DNA vaccines that call to dendritic cells. J. Clin. Invest. **114:**1241–1244.
22. **Langermann, S., S. Palaszynsky, A. Sadzience, C. Stover, and S. Koenig.** 1994. Systemic and mucosal immunity induced by BCG vector expressing outer-surface protein A of *Borrelia burgdorferi*. Nature **372:**552–555.
23. **Lewis, D. J. M., et al.** 2009. Transient facial nerve paralysis (Bell's palsy) following intranasal delivery of a genetically detoxified mutant of *Escherichia coli* heat labile toxin. PLoS One. **4**(9):e6999.
24. **Maraskovsky, E., et al.** 1996. Dramatic increase in the numbers of functionally mature dendritic cells in Flt3 ligand-treated mice: multiple dendritic cell subpopulations identified. J. Exp. Med. **184:**1953–1962.
25. **McGhee, J. R., et al.** 1992. The mucosal immune system: from fundamental concepts to vaccine development. Vaccine **10:**75–88.
26. **Mestecky, J., R. S. Blumberg, H. Kiyono, and J. R. McGhee.** 2003. The mucosal immune system, p. 965–1020. *In* W. E. Paul, (ed.), Fundamental immunology, 5th ed. Lippincott Williams & Wilkins, Philadelphia, PA.
27. **Moreno, A. T., et al.** 2010. Immunization of mice with single PspA fragments induces antibodies capable of mediating complement deposition on different pneumococcal strains and cross-protection. Clin. Vaccine Immunol. **17:**439–446.
28. **Musher, D. M., A. M. Rueda, M. H. Nahm, E. A. Gravis, and M. C. Rodriguez-Barradas.** 2008. Initial and subsequent response to pneumococcal polysaccharide and protein-conjugate vaccines administered sequentially in adults who have recovered from pneumococcal pneumonia. J. Infect. Dis. **198:**1019–1027.
29. **Mutsch, M., et al.** 2004. Use of the inactivated intranasal influenza vaccine and the risk of Bell's palsy in Switzerland. N. Engl. J. Med. **350:**896–903.
30. **Ren, B. A., J. Szalai, S. K. Hollingshead, and D. E. Briles.** 2004. Effects of PspA and antibodies to PspA on activation and deposition of complement on the pneumococcal surface. Infect. Immun. **72:**114–122.
31. **Roche, A. M., and J. N. Weiser.** 2010. Identification of the targets of cross-

reactive antibodies induced by *Streptococcus pneumoniae* colonization. Infect. Immun. **78:**2231–2239.
32. **Sekine, S., et al.** 2008. A novel adenovirus expressing Flt3 ligand enhances mucosal immunity by inducing mature nasopharyngeal-associated lymphoreticular tissue dendritic cell migration. J. Immunol. **180:**8126–8134.
33. **Sen, D., L. Forrest, T. B. Kepler, I. Parker, and M. D. Cahalan.** 2010. Selective and site-specific mobilization of dermal dendritic cells and langerhans cells by Th1- and Th2-polarizing adjuvants. Proc. Natl. Acad. Sci. U. S. A. **107:**8334–8339.
34. **Shao, Z., A. S. Bharadwaj, H. S. McGee, T. L. Makinde, and D. K. Agrawal.** 2009. Flt-3 ligand increases a lung dendritic cell subset with regulatory properties in allergic airway inflammation. J. Allergy Clin. Immunol. **123:** 917–924.
35. **Shao, Z., T. O. Makinde, H. S. McGee, X. Wang, and D. K. Agrawal.** 2009. Fms-like tyrosine kinase 3 ligand regulates migratory pattern and antigen uptake of lung dendritic cell subsets in a murine model of allergic airway inflammation. J. Immunol. **183:**7531–7538.
36. **Takahashi, E., et al.** 2010. Attenuation of inducible respiratory immune responses by oseltamivir treatment in mice infected with influenza A virus. Microbes Infect. **12:**778–783.
37. **Tart, R. C., L. S. McDaniel, B. A. Ralph, and D. E. Briles.** 1996. Truncated *Streptococcus pneumoniae* PspA molecules elicit cross-protective immunity against pneumococcal challenge in mice. J. Infect. Dis. **173:**380–386.
38. **Triccas, J. A., et al.** 2007. Effects of DNA- and *Mycobacterium bovis* BCG-based delivery of the Flt3 ligand on protective immunity to *Mycobacterium tuberculosis*. Infect. Immun. **75:**5368–5375.
39. **Vadolas, J., J. K. Davies, P. J. Wright, and R. A. Strugnell.** 1995. Intranasal immunization with liposomes induces strong mucosal immune responses in mice. Eur. J. Immunol. **25:**969–975.
40. **van Ginkel, F. W., R. J. Jackson, Y. Yuki, and J. R. McGhee.** 2000. Cutting edge: the mucosal adjuvant cholera toxin redirects vaccine proteins into olfactory tissues. J. Immunol. **165:**4778–4782.
41. **Vitharsson, G., I. Jonsdottir, S. Jonsson, and H. Valdimarsson.** 1994. Opsonization and antibodies to capsular and cell wall polysaccharides of *Streptococcus pneumoniae.* J. Infect. Dis. **170:**592–599.
42. **Wu, H. Y., M. H. Nahm, Y. Guo, M. W. Russell, and D. E. Briles.** 1997. Intranasal immunization of mice with PspA (pneumococcal surface protein A) can prevent intranasal carriage, pulmonary infection, and sepsis with *Streptococcus pneumoniae.* J. Infect. Dis. **175:**839–846.

Editor: A. Camilli

MICROBIOLOGY LETTERS

RESEARCH LETTER

Identification of the *Vibrio parahaemolyticus* type III secretion system 2-associated chaperone VocC for the T3SS2-specific effector VopC

Yukihiro Akeda[1,2], Toshio Kodama[1], Kazunobu Saito[3,4], Tetsuya Iida[5], Kazunori Oishi[2] & Takeshi Honda[1]

[1]Department of Bacterial Infections, Research Institute for Microbial Diseases, Osaka University, Osaka, Japan; [2]Laboratory of Clinical Research on Infectious Diseases, International Research Center for Infectious Diseases, Research Institute for Microbial Diseases, Osaka University, Osaka, Japan; [3]Central Instrumentation Laboratory, Research Institute for Microbial Diseases, Osaka University, Osaka, Japan; [4]DNA-Chip Development Center for Infectious Diseases, Research Institute for Microbial Diseases, Osaka University, Osaka, Japan; and [5]Laboratory of Genomic Research on Pathogenic Bacteria, International Research Center for Infectious Diseases, Research Institute for Microbial Diseases, Osaka University, Osaka, Japan

Correspondence: Yukihiro Akeda, Laboratory of Clinical Research on Infectious Diseases, International Research Center for Infectious Diseases, Research Institute for Microbial Disease, Osaka University, Osaka, Japan. Tel.: +81 6 6879 4253; fax:+81 6 6879 4255; e-mail: akeda@biken.osaka-u.ac.jp

Received 13 May 2011; revised 24 August 2011; accepted 24 August 2011.
Final version published online 21 September 2011.

DOI: 10.1111/j.1574-6968.2011.02399.x

Editor: Peter Lund

Keywords
Vibrio parahaemolyticus; type III secretion system; chaperone.

Abstract

The enteropathogen *Vibrio parahaemolyticus* possesses two sets of type III secretion systems, T3SS1 and T3SS2. Effector proteins secreted by these T3SSs are delivered into host cells, leading to cell death or diarrhea. However, it is not known how specific effectors are secreted through a specific T3SS when both T3SSs are expressed within bacteria. One molecule thought to determine secretion specificity is a T3SS-associated chaperone; however, no T3SS2-specific chaperone has been identified. Therefore, we screened T3SS2 chaperone candidates by a pull-down assay using T3SS2 effectors fused with glutathione-S-transferase. A secretion assay revealed that the newly identified cognate chaperone VocC for the T3SS2-specific effector VopC was required for the efficient secretion of the substrate through T3SS2. Further experiments determined the chaperone-binding domain and the amino-terminal secretion signal of the cognate effector. These findings, in addition to the previously identified T3SS1-specific chaperone, VecA, provide a strategy to clarify the specificity of effector secretion through T3SSs of *V. parahaemolyticus*.

Introduction

Vibrio parahaemolyticus is a major causative agent of gastroenteritis after the consumption of raw seafood. A genomic analysis of this organism revealed two sets of type III secretion systems, T3SS1 and T3SS2 (Makino *et al.*, 2003), and functional assays were carried out to examine the contribution of each T3SS to the pathogenicity of *V. parahaemolyticus* (Park *et al.*, 2004; Ono *et al.*, 2006; Hiyoshi *et al.*, 2010; Pineyro *et al.*, 2010). The results indicated that the enterotoxicity of this bacterium in humans was dependent on T3SS2. The genes encoding for T3SS2 are located within the *V. parahaemolyticus* pathogenicity island (Vp-PAI) (Sugiyama *et al.*, 2008) that causes fluid accumulation in a rabbit ileal loop model (Park *et al.*, 2004; Hiyoshi *et al.*, 2010), and it has been confirmed that T3SS2 causes diarrhea in a piglet model (Pineyro *et al.*, 2010).

Many Gram-negative bacteria utilize the T3SS to efficiently manipulate their hosts by injecting virulence factors, so-called effectors, into host cells (Coburn *et al.*, 2007; Galan, 2009). Protein secretion by T3SS is cooperatively regulated by the control of transcription of T3SS effectors/components, and at the post-transcriptional level (Francis *et al.*, 2002; Yahr & Wolfgang, 2006). Previous studies have shown that the T3SS effector/chaperone complex is indispensable for the efficient delivery of effectors into host cells (Galan & Wolf-Watz, 2006), as hypothesized in the model of the protein secretion mechanism (Arnold *et al.*, 2009). The established model is based on a single T3SS apparatus present in one bacterium, and questions have arisen as to how the destination of effectors is determined in a bacterium equipped with multiple T3SSs. There are several bacteria with multiple T3SSs, including *Salmonella* (Knodler *et al.*, 2002),

enterohemorrhagic *Escherichia coli* (Hartleib *et al.*, 2003), *Burkholderia pseudomallei* (Attree & Attree, 2001), and *V. parahaemolyticus* (Makino *et al.*, 2003). Of these, *V. parahaemolyticus* is the best model for exploring the specificity of protein secretion mechanisms in the presence of multiple T3SSs because *V. parahaemolyticus* can specifically secrete multiple effectors via two individual T3SSs under the same culture conditions (Akeda *et al.*, 2009). Based on the current model of protein secretion through the T3SS, T3SS-specific chaperones or the amino-terminal secretion signal sequence of secreted effectors could be the determinant of the specificity of effector secretion via individual apparatuses (Arnold *et al.*, 2009). The specificity of effector secretion through *Salmonella* pathogenicity island-1 (SPI-1) or the flagellar system is dependent on the T3SS chaperones of the secreted effectors (Lee & Galan, 2004). However, the requirements for specificity in nonflagellar-type T3SSs for the secretion of T3SS effectors in the same bacterial cell have not been investigated. In *V. parahaemolyticus*, there are a number of T3SS1- and 2-specific effectors. The T3SS2-specific effectors include VopP (Park *et al.*, 2004) (also known as VopA) (Trosky *et al.*, 2004), VopT (Kodama *et al.*, 2007), VopL (Liverman *et al.*, 2007), and VopC (Kodama *et al.*, 2007, 2008). The T3SS1-specific effectors include VepA (Akeda *et al.*, 2009) (also known as VopQ) (Burdette *et al.*, 2009) and VepB (Akeda *et al.*, 2009) (also known as VopS) (Yarbrough *et al.*, 2009). Only one T3SS-specific chaperone, VecA, has been identified, which is for the T3SS1 effector VepA (Akeda *et al.*, 2009), but no chaperone for T3SS2 effectors has been identified. Therefore, the T3SS2-specific chaperone must be identified before undertaking experiments to examine the hypothesized effector specificity of *V. parahaemolyticus* T3SSs. In this study, we screened possible T3SS2-specific chaperones and successfully identified VocC, which is a T3SS2-specific chaperone for the T3SS2-specific effectors VopC and, presumably, VopT and VopL.

Materials and methods

Bacterial strains and growth conditions

The derivative strain POR-1 (Δ*tdhAS*) of the sequenced *V. parahaemolyticus* strain RIMD2210633 was used as the wild type in this study (Park *et al.*, 2004). The T3SS1 (Δ*vcrD1*), T3SS2 (Δ*vcrD2*), VepA (Δ*vepA*), VopC (Δ*vopC*), VopP (Δ*vopP*), VopL (Δ*vopL*), and VopT (Δ*vopT*) knockout strains of *V. parahaemolyticus* have been reported previously (Park *et al.*, 2004; Ono *et al.*, 2006; Kodama *et al.*, 2007; Kodama *et al.*, 2008). All *V. parahaemolyticus* strains were grown in high-salt Luria–Bertani (LB) medium (1% Bacto tryptone, 0.5% yeast extract, and 3% NaCl) at 37 °C for routine culture. For the T3SS-inducing conditions, strains were grown in LB medium (1% Bacto tryptone, 0.5% yeast extract, and 0.5% NaCl). The *E. coli* strains DH5α, SM10λ*pir*, and BL21 (DE3) were used for the general manipulation of DNA, the mobilization of the suicide vector into *V. parahaemolyticus*, and protein purification, respectively. The *E. coli* strains were also grown in LB medium. When necessary, media were supplemented with the following antibiotics: ampicillin (100 μg mL^{-1}), chloramphenicol (25 μg mL^{-1}), kanamycin (50 μg mL^{-1}), or tetracycline (5 μg mL^{-1}).

Screening of T3SS2-specific chaperone candidates

Because *V. parahaemolyticus* is naturally resistant to ampicillin, the plasmid pGEX-6P-1-Cm (Cm^r, Ap^s) was constructed through the insertion of a chloramphenicol resistance gene (*cat*) from pACYC184 into the ampicillin resistance gene (*bla*) on pGEX-6P-1 (GE Healthcare Bio-Sciences). The amino-terminal 1–200 amino acids of the T3SS2 effectors (VopC, VopL, VopP, and VopT) were fused to glutathione-S-transferase (GST) in pGEX-6P-1-Cm. These plasmids were then transformed into the strain in which the gene for the respective effector was deleted. After incubation under T3SS-inducing conditions, bacterial pellets were collected and lysed using lysis buffer (20 mM Tris HCl, 200 mM NaCl, 2 mM dithiothreitol, and 0.1% Triton X-100, pH 8.0) containing 10 mg mL^{-1} of lysozyme, 10 mg mL^{-1} of RNase, and 5 U of DNase I. Lysates were centrifuged at 20 000 *g* for 20 min. The cleared supernatant was applied to a Glutathione Sepharose 4 Fast Flow column (GE Healthcare Bio-Sciences) equilibrated with lysis buffer. After washing the column with washing buffer (20 mM Tris HCl, 500 mM NaCl, and 2 mM dithiothreitol, pH 8.0), the amino termini of the T3SS2 effectors were eluted using elution buffer (20 mM Tris HCl, 200 mM NaCl, and 10 mM glutathione, pH 8.0). Eluted samples were used for the identification of proteins that copurified with the amino termini of T3SS2 effectors.

Sample preparation and liquid chromatography–tandem mass spectrometry (LC–MS/MS) analysis

Protein samples were separated using sodium dodecyl sulfate polyacrylamide gel electrophoresis (SDS-PAGE) followed by silver staining. Protein bands were excised from the gel and digested *in situ* using Trypsin Gold (Promega). The digested samples were analyzed using nanocapillary reverse-phase LC–MS/MS using a C18 column (φ 75 μm) on a nanoLC system (Ultimate; LC

Packings) coupled to a quadrupole time-of-flight mass spectrometer (QTOF Ultima; Waters). Direct injection data-dependent acquisition was performed using one MS channel for every three MS/MS channels and dynamic exclusion for selected ions. Proteins were identified through searching databases using Mascot Server (Matrix Science).

Construction of the Δ*vocC* strain and isogenic mutant strains encoding the *vopC–cyaA* translational fusion

The Δ*vocC* strain of *V. parahaemolyticus* POR-1 was constructed as described previously (Kodama *et al.*, 2002; Ono *et al.*, 2006) using the following specific primers: Δ*vocC*-1: 5′-GGCCGGATCCCAATACCTTGAATAAGTAC CGAGTGTTATATAAG-3′; Δ*vocC*-2: 5′-CTACATAGATA TTAGTTATAGTTTCACTTCAGAAGCCCGCAGTGTTCT CATATTGATTCCTTG-3′; Δ*vocC*-3: 5′-CAAGGAATCAA TATGAGAACACTGCGGGCTTCTGAAGTGAAA CTATA ACTAATATCTATGTAG-3′; and Δ*vocC*-4: 5′-CCGGCTG CAGGCATGACGTAGCCATTAACGTATCAATTAAAGG-3′. The resultant plasmid in *E. coli* SM10λ*pir* was used for homologous recombination in *V. parahaemolyticus*. Isogenic mutants encoding the gene for the translational fusion $VopC_{1\ 30}$–$CyaA_{2\ 405}$ (*Bordetella* adenylate cyclase) in wild-type and Δ*vocC* strains were constructed by homologous recombination using pYAK1.

Secretion assay

Bacterial culture was maintained under T3SS-inducing conditions at 37 °C. After a 3-h incubation, the bacterial culture was separated into culture supernatants and bacterial pellets using centrifugation. The supernatant was filtered through a 0.22-μm-pore filter, and 10% sodium deoxycholate and ice-cold 100% trichloroacetate were then added to a final concentration of 0.1% and 10%, respectively. Samples were kept on ice for 1 h and then centrifuged at 21 000 *g* for 20 min at 4 °C. Precipitates were washed with ice-cold acetone followed by centrifugation. The resulting precipitates and bacterial pellets were analyzed using SDS-PAGE before Western blotting using rabbit antisera against VopC, VopL, VopD1, or VopD2. The antibody against GroEL was purchased from MBL (Nagoya, Japan).

RNA isolation and reverse transcription-polymerase chain reaction (RT-PCR)

Vibrio parahaemolyticus strains were grown under T3SS-inducing conditions for 3 h. After the incubation, the bacteria were collected and RNA was isolated using the RNeasy Mini kit (Qiagen). RNA purification was followed by reverse transcription using Superscript III (Invitrogen) and random hexamers (Takara Bio). Semi-quantitative PCR was carried out using primers targeted to the internal fragments of *vopC* (*vopC*-1 5′-AGCAGCGTGGTGG TTAGTGAATCCAACCAA-3′ and *vopC*-2 5′-TAGAACA ATAGTCTATCAAACCCTGAATAC-3′), *vopD2* (*vopD2*-1 5′-CGATGCTGAACGAGCGTGCGTCGCAATTGG-3′ and *vopD2*-2 5′-GAGGGTCTCAAACGAATGAGCAACCGAAC G-3′), and *vocC* (*vocC*-1 5′-ATGAGAACACTGCGAGAAA TCGTGTACAAAAC-3′ and *vocC*-2 5′-TTATAGTTTCACT TCAGAAGCCATTTTATTAAATAAAG-3′). The PCR conditions were as follows: one cycle at 98 °C for 3 min; 30 cycles at 98 °C for 10 s, 53 °C for 30 s, and 72 °C for 1 min; and one cycle at 72 °C for 7 min. The PCR products were analyzed using 2% agarose gel electrophoresis.

Purification of recombinant GST–VocC and VopC–HIS

VocC fused to GST was expressed using pGEX-6P-1 (GE Healthcare Bio-Sciences) encoding the *vocC* gene amplified by PCR. The *E. coli* strain BL21 (DE3) harboring the VocC-expressing plasmid was grown in 2×yeast extract and tryptone (YT) medium (1.6% Bacto tryptone, 1% yeast extract, and 0.5% NaCl) for 18 h at 37 °C and then subcultured in 2× YT medium for 3 h at 37 °C. After the addition of isopropyl beta-D-1-thiogalactopyranoside (IPTG) at a final concentration of 1 mM, the bacterial culture was incubated for 4 h at 37 °C. Further purification was carried out following the protocol described in the 'Screening of T3SS2-specific chaperone candidates' section. Purified GST–VocC did not show any other bands using SDS-PAGE and Coomassie staining, except for a small amount of breakdown product.

VopC fused to a poly-histidine tag (HIS) was expressed using pET28a (Novagen) encoding *vopC* amplified using PCR. The *E. coli* strain BL21 (DE3) harboring the VopC-expressing plasmid was grown under similar conditions as GST–VocC. The purification of VopC–HIS was carried out using Ni-NTA HIS Bind beads (Novagen) according to the manufacturer's instructions. Purified VopC–HIS did not show any other bands using SDS-PAGE and Coomassie staining, except for a small amount of breakdown product.

Pull-down assay using GST–VocC and VopC–HIS or VopC–CyaA

Purified GST–VocC (4 mM) was mixed with glutathione beads equilibrated with TBST (20 mM Tris HCl, 200 mM NaCl, and 0.05% Tween 20, pH 8.0). After washing the beads with TBST to remove unbound GST–VocC, purified VopC–HIS (4 mM) or *E. coli* lysates (from 100 mL

cultures in 2× YT medium) expressing a series of truncated VopC fused with CyaA (*Bordetella* adenylate cyclase) were added to the beads suspended in TBST. Following incubation at 4 °C with rotation, the beads were washed extensively with TBST and separated using SDS-PAGE, followed by Western blotting. Anti-GST (Cell Signaling), anti-poly-histidine tag (Sigma-Aldrich), and anti-CyaA (Santa Cruz Biotechnology) antibodies were used to detect the respective target proteins on the membrane.

Translocation assay using VopC fused with CyaA

The human colon adenocarcinoma cell line Caco-2 was used for the translocation assay. Caco-2 cells were infected with *V. parahaemolyticus* strains expressing VopC C-terminally fused with the catalytic domain of CyaA at 37 °C in a 5% CO_2 atmosphere. After a 3-h incubation, Caco-2 cells were washed with PBS, and intracellular cAMP levels were measured using the cAMP Biotrak enzyme immunoassay system (GE Healthcare Bio-Science) according to the manufacturer's instructions. All data are expressed as the means and standard deviations of three determinations per experimental condition. Statistical significance was determined using a one-way ANOVA followed by Dunnett's multiple comparison test. A P-value < 0.05 was considered statistically significant.

Results

Screening of T3SS2-associated chaperone candidates

The T3SS-associated chaperone and the effector complex bind to each other with high affinity (Luo *et al.*, 2001). Therefore, we used a screening assay using T3SS2 effectors fused with GST to pull down chaperone candidates. The amino-terminal regions of T3SS2 effectors (VopC, VopL, VopP, and VopT) fused to the CyaA (*Bordetella pertussis* toxin) catalytic domain can be injected into host cells (Kodama *et al.*, 2007) (T. Kodama, unpublished data). This is consistent with other T3SS effectors and suggests that the amino-terminal regions of *V. parahaemolyticus* T3SS2 effectors are sufficient for efficient secretion and translocation. In general, amino-terminal domains (1–200 amino acids) of T3SS effectors contain the amino-terminal secretion signal of the T3SS and the chaperone-binding domains, which are both essential for effector secretion (Feldman & Cornelis, 2003; Parsot *et al.*, 2003). Plasmids expressing the amino-terminal domains (1–200 amino acids) of the T3SS2 effectors VopC, VopL, VopP, and VopT fused to GST were introduced into *V. parahaemolyticus* knockout strains for each gene. The GST fusions expressed in *V. parahaemolyticus* strains were purified using glutathione beads and separated using SDS-PAGE. The molecular weights of most T3SS-associated chaperones are less than 20 kDa (Feldman & Cornelis, 2003; Parsot *et al.*, 2003); therefore, the areas containing proteins of these molecular weights were carefully observed. Although the T3SS2 effectors fused to GST appeared to be unstable (a lower amount of T3SS2 effector fusions than breakdown products was observed), the amino-terminal 1–200 amino acids of the T3SS2 effectors fused to GST were copurified with a specific band that was not observed in the negative control (GST alone), as shown in Fig. 1a. Mass analysis revealed proteins interacting with GST–$VopC_{1\ 200}$, GST–$VopL_{1\ 200}$, and GST–$VopT_{1\ 200}$ (Fig. 1b), while GST–$VopP_{1\ 200}$ did not interact with any specific proteins that could be chaperone candidates. The results suggested that only one protein encoded in the Vp-PAI, VPA1334 (designated VocC; Vop chaperone C), appeared to be a T3SS chaperone candidate. The molecular weight and the isoelectric point of VocC were estimated as 14.3 kDa and 5.41, respectively. Based on the information from previously identified T3SS-associated chaperones (Feldman & Cornelis, 2003; Parsot *et al.*, 2003), these values indicate that VocC is a possible T3SS2-associated chaperone for VopC, VopL, and VopT, and this result may categorize VocC as a type IB class chaperone, which chaperones multiple effectors (Parsot *et al.*, 2003).

VocC is required for the efficient secretion of VopC via T3SS2

To examine the chaperone activity of VocC, we tested whether VocC was required for effector secretion, specifically VopC, through T3SS2. A secretion assay showed the secretion of VopC in the wild type and the Δ*vocC* strain complemented with a *vocC* complementation plasmid (p*vocC*) (Fig. 2a). In contrast, VopC was not observed in the supernatant or the bacterial pellet of the *vocC* knockout strain (Δ*vocC*). VopL, which was also found to interact with VocC in the screening assay, was not visible in the supernatant of Δ*vocC*, as assayed by Western blotting using an anti-VopL antibody (Fig. 2a). Although faint bands were detected in all samples using an anti-VopL antibody, these bands were confirmed to be nonspecific using the Δ*vopL* mutant strain (data not shown). To evaluate the possibility that the absence of VopC in the supernatant of Δ*vocC* was caused by a small amount of VopC expressed in the bacterial pellets, we introduced a plasmid encoding *vopC* into the Δ*vocC* strain. As shown in Fig. 2a, although overexpressed VopC was detected in bacterial pellets, it was not detected in the supernatant. To examine whether VocC might be required by all T3SS systems for protein secretion, VopD1 (T3SS1 translocon) and VopD2 (T3SS2 translocon) were probed using

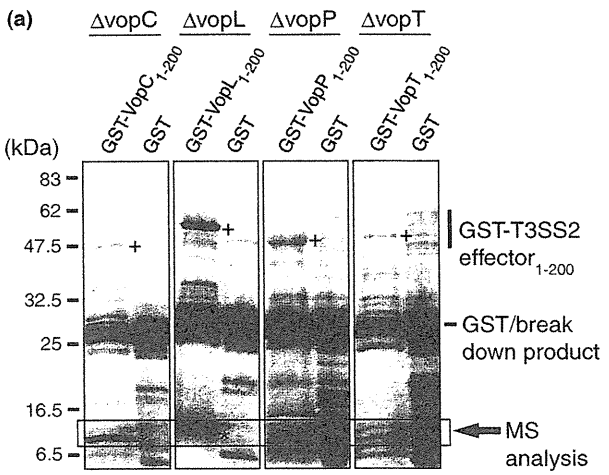

(b)

Effector	Identified protein	MW	Score
$VopC_{1-200}$	Hypothetical protein (VocC)	14 323	362
	VopC	40 622	122
	Preprotein translocase subunit YajC	11 832	50
$VopL_{1-200}$	Hypothetical protein (VocC)	14 323	502
	30S ribosomal protein S10	11 713	155
$VopP_{1-200}$	30S ribosomal protein S10	11 713	139
	VopP	32 925	51
$VopT_{1-200}$	Hypothetical protein (VocC)	14 323	235
	30S ribosomal protein S10	11 713	103
	50S ribosomal protein L22	13 995	78

Fig. 1. Screening of candidate chaperones for T3SS2 effectors. Plasmids expressing GST–$VopC_{1-200}$, GST–$VopL_{1-200}$, GST–$VopP_{1-200}$, GST–$VopT_{1-200}$, or GST alone (as a negative control) were transformed into the respective effector-deficient strains (Δ*vopC*, Δ*vopL*, Δ*vopP*, or Δ*vopT*) of *Vibrio parahaemolyticus*. Overexpressed GST fusion proteins from each strain were isolated using glutathione sepharose. Elutions were separated using SDS-PAGE and silver-stained. (a) Silver staining of purified proteins from each strain. A rectangular area indicates the samples used for MS analysis. Asterisks indicate a band specific to GST–$VopC_{1-200}$, GST–$VopT_{1-200}$, or GST–$VopL_{1-200}$ elutions in comparison with GST-only samples. The '+' indicates the amino-terminal 200 amino acids of T3SS2 effectors fused with GST. (b) Proteins identified from specific bands copurified with GST–T3SS2 effectors. The molecular weights and scores determined using a Mascot search are shown.

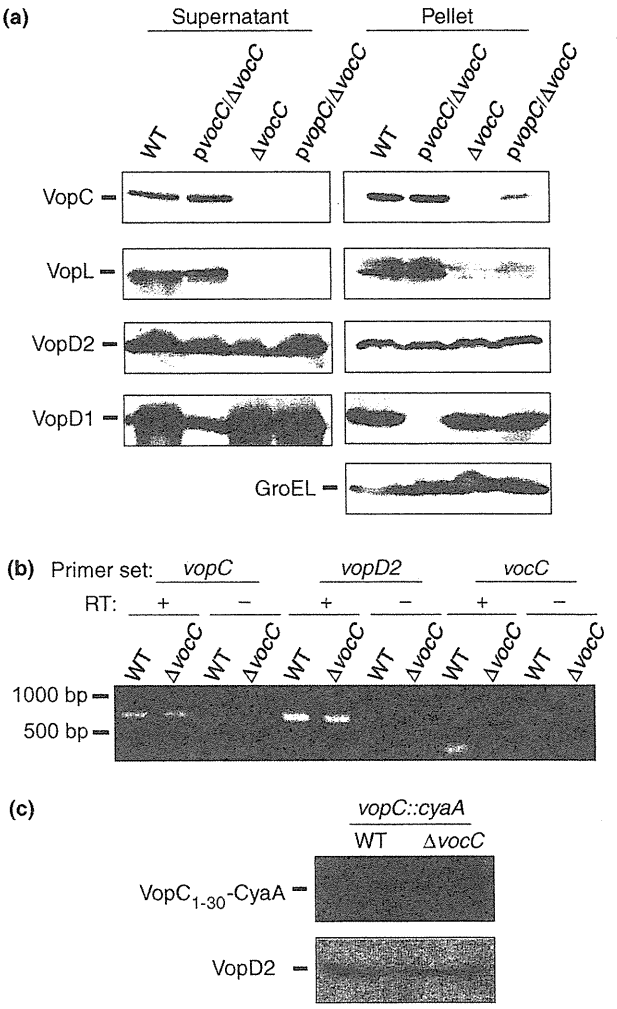

Fig. 2. VocC is required for VopC secretion. (a) Secretion assay of *Vibrio parahaemolyticus* strains. *Vibrio parahaemolyticus* strains [wild type, Δ*vocC*, Δ*vocC* complemented with a plasmid encoding *vocC* (p*vocC*/Δ*vocC*) and Δ*vocC* carrying the plasmid encoding *vopC* (p*vopC*/Δ*vocC*)] were grown under T3SS-inducing conditions. Culture supernatants and bacterial pellets were Western-blotted, and proteins were detected using rabbit polyclonal antibodies against VopC, VopL, VopD2 (T3SS2-specific protein), and VopD1 (T3SS1-specific protein). GroEL was detected to confirm that an equivalent amount of protein was loaded in each bacterial pellet. (b) RT-PCR of *vopC*, *vopD2*, and *vocC* in *Vibrio parahaemolyticus* strains. Amplification was performed using cDNA (RT+) or RNA (RT−) extracted from wild-type and Δ*vocC* strains of *Vibrio parahaemolyticus*. The absence of genomic DNA contamination was confirmed by PCR using RNA without reverse transcription (RT−). The primers for *vopD2* and *vocC* were used as positive and negative controls, respectively. (c) The expression of the $VopC_{1-30}$–CyaA translational fusion in *Vibrio parahaemolyticus* strains (WT and Δ*vocC*) carrying the gene encoding $VopC_{1-30}$–CyaA. Strains were grown under T3SS-inducing conditions. $VopC_{1-30}$–CyaA was detected in bacterial pellets by Western blotting using an anti-CyaA monoclonal antibody. VopD2 was detected as an internal control using an anti-VopD2 antibody.

antisera against VopD1 and VopD2, respectively. The secretion of VopD1 and VopD2 by T3SS1 or T3SS2 was observed in the *vocC* mutant, and a lower level of VopD1 was observed in the cell pellet of the *vocC*-complemented Δ*vocC* strain. The transcriptional regulation of T3SS2 and T3SS1 is influenced by each other, especially with the addition of bile (Gotoh *et al.*, 2010); these results might explain our observation of a lower level of VopD1 in the *vocC*-complemented Δ*vocC* strain.

Some T3SS-associated chaperones can regulate the transcription of T3SS-associated genes (Darwin & Miller,

2001; Pilonieta & Munson, 2008). Therefore, it was possible that VocC regulated the transcription of VopC because lower levels of VopC protein were observed in the supernatant and the bacterial pellet in the secretion assay. The transcriptional level of *vopC* in the Δ*vocC* strain was evaluated using semi-quantitative RT-PCR. The levels of both *vopC* and *vopD2* were indistinguishable between wild-type and Δ*vocC* strains grown under T3SS-inducing conditions (Fig. 2b). Moreover, the translational level of *vopC* in the Δ*vocC* strain was evaluated using a translational fusion to amino acids 2–405 of CyaA from *B. pertussis*. The isogenic mutants of $VopC_{1-30}$–CyaA in the wild-type and Δ*vocC* strains expressed a similar level of the translational fusion under the same conditions as the secretion assay (Fig. 2c).

Similar transcriptional and translational levels of *vopC* in both wild-type and Δ*vocC* strains indicated that the decreased protein level of VopC in the absence of VocC might be caused by the degradation of VopC.

From these results, it appears that VocC does not play a role in regulating the transcription/translation of VopC and that VocC is the chaperone necessary for the secretion of VopC through T3SS2.

The translocation of VopC is dependent on its cognate chaperone VocC

The translocation of T3SS effectors into host cells is the most distinctive function of T3SSs. However, the secretion of T3SS effectors is thought to be a different event from translocation (Lee & Galan, 2004) because there are several examples of exceptions in which constructs of the amino-terminal signal sequence of T3SS effectors fused with a reporter protein can be observed in the supernatant and not inside host cells (Lee & Galan, 2004). To exclude this possibility for VocC, a translocation assay using VopC fused with the catalytic domain of CyaA was performed (Sory *et al.*, 1995). This assay determines whether a T3SS effector–CyaA fusion is injected into eukaryotic cells by measuring intracellular cAMP levels because the activity of the CyaA catalytic domain requires calmodulin within eukaryotic cells. The wild-type strain expressing the VopC–CyaA fusion induced a high level of cAMP inside Caco-2 cells, while the Δ*vocC* strain did not, producing levels similar to the negative control (the T3SS2-deficient strain, *vcrD2*) (Fig. 3). These results indicate that VocC is necessary for not only the secretion of VopC but also its translocation into host cells.

Binding of VopC to its cognate chaperone VocC

Another characteristic of T3SS chaperones is the ability to bind their cognate effector. As expected from the screening assay used to identify T3SS2-associated chaperones (Fig. 1), VocC appeared to bind VopC. In this binding experiment, purified proteins were used to observe direct binding between the chaperone and an effector. A pull-down assay was performed using purified GST–VocC (42.6 kDa) and poly-histidine-tagged VopC (VopC–HIS; 45.9 kDa). As shown in Fig. 4, GST–VocC coprecipitated with VopC–HIS, while GST alone as a negative control did not. Another presumable substrate for VocC, VopT, fused with a poly-histidine tag showed similar binding results to GST–VocC (data not shown).

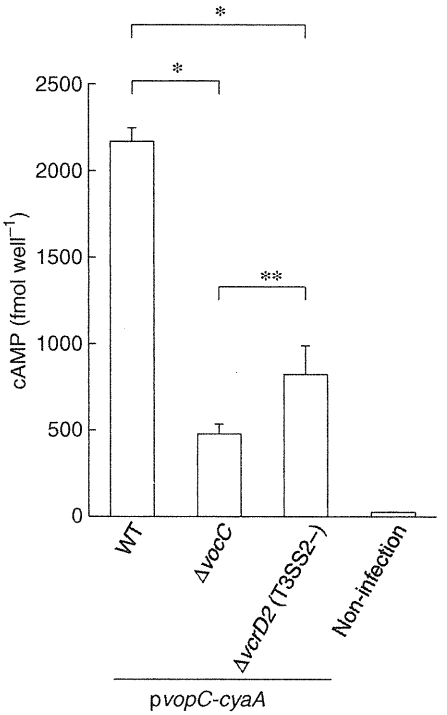

Fig. 3. VocC is required for the translocation of VopC. Translocation assay using VopC fused with the reporter protein CyaA. *Vibrio parahaemolyticus* strains (wild-type, Δ*vocC*, or Δ*vcrD2* strains in a Δ*vopC* background) harboring the plasmid encoding *vopC–cyaA* were added to Caco-2 cells (MOI = 10). After 3 h of infection, cultured cells were washed with PBS to remove bacteria, and the levels of intracellular cAMP were measured using an ELISA. The level of intracellular cAMP was used as the index of VopC translocation into Caco-2 cells. All data are expressed as means and standard deviations of three independent experiments. $*P < 0.05$, $**P > 0.05$.

Determination of the VocC-binding site and secretion signal in VopC

In previous studies, the binding of T3SS-associated chaperones and effectors and the amino-terminal secretion signal of effectors were required for efficient secretion via the T3SS (Arnold *et al.*, 2009). Therefore, it was important to identify the chaperone-binding domain and the

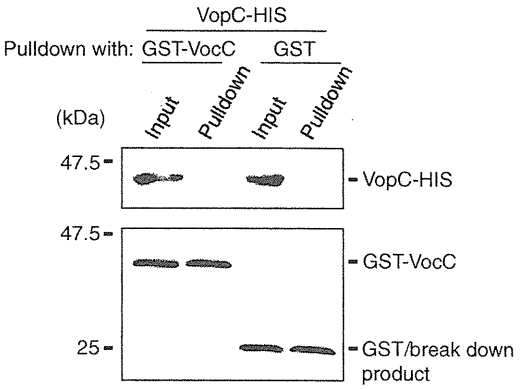

Fig. 4. VocC binds to VopC. Pull-down assay between GST–VocC and VopC–HIS. Purified GST–VocC (4 mM) or GST alone (4 mM) was pre-absorbed with glutathione beads and mixed (molar ratio 1 : 1) with purified VopC tagged with poly-histidine (4 mM). Input samples (Input) and washed beads (Pulldown) were Western-blotted to detect fusion proteins using anti-GST and anti-poly-histidine-tagged antibodies.

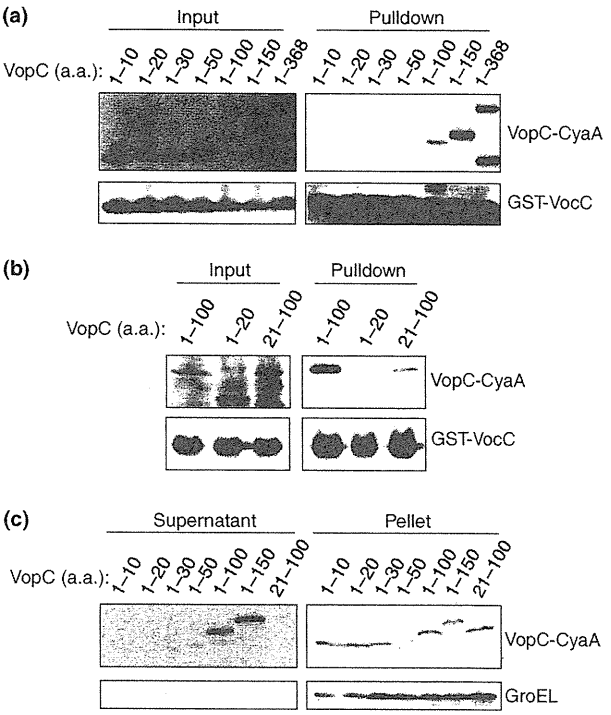

Fig. 5. Identification of VocC-binding domain and amino-terminal secretion signal in VopC. (a) Pull-down assay between GST–VocC and VopC–CyaA. Whole *Escherichia coli* lysates expressing a series of truncated VopC–CyaA fusion proteins were applied to glutathione beads pre-absorbed with GST–VocC. After washing the beads to remove unbound VopC–CyaA fusions, input samples (Input) and washed beads (Pulldown) were analyzed using SDS-PAGE separation followed by Western blotting using anti-GST and anti-CyaA antibodies. (b) Pull-down assay between GST–VocC and $VopC_{21-100}$–CyaA. The assay was carried out as described in (a) using $VopC_{21-100}$-CyaA. Separated proteins were detected using anti-CyaA and anti-GST antibodies. (c) Secretion of VopC–CyaA fusions. A series of truncated VopC–CyaA fusion proteins was expressed in Δ*vopC* strains in a *Vibrio parahaemolyticus* T3SS1-knockout (Δ*vcrD1*) background. After incubation for 3 h under T3SS-inducing conditions, culture supernatants and bacterial pellets were collected and analyzed using SDS-PAGE separation followed by Western blotting using anti-CyaA and anti-GroEL as a marker for the leakage of cytoplasmic proteins.

amino-terminal secretion signal of VopC. First, we used a series of truncated VopC mutants fused with CyaA in a pull-down assay with GST–VocC. As shown in Fig. 5a, the domain covering at least 100 amino acids from the amino terminus of VopC was responsible for binding to VocC. Additional pull-down assays using $VopC_{21\ 100}$–CyaA showed that VocC bound to the amino-terminal 21–100 amino acids of VopC (Fig. 5b). Next, we examined whether an amino-terminal secretion signal existed in VopC. A secretion assay using *V. parahaemolyticus* T3SS1-deficient strains (Δ*vcrD1*) expressing a series of truncated VopC mutants fused with CyaA was carried out to assess the specific secretion of VopC fusions through T3SS2 (Fig. 5c). The secretion assay showed a strong signal for $VopC_{1\ 100}$–CyaA and $VopC_{1\ 150}$–CyaA on the membrane and weak signals for fusion proteins containing at least amino acids 1–20 of the amino terminus of VopC. This result indicates that the efficient secretion of VopC via T3SS2 requires both the chaperone-binding domain (21–100 amino acids) and the amino-terminal secretion signal (1–20 amino acids), which was confirmed by no secretion of $VopC_{21\ 100}$–CyaA in this assay.

Discussion

In this study, we identified the T3SS2-associated chaperone VocC for the T3SS2-specific effector VopC and, presumably, VopL and VopT using T3SS effectors fused with GST and determined the chaperone-binding domain and the amino-terminal secretion signal in VopC. These results, in addition to the previously identified T3SS1-associated chaperone VecA (for the T3SS1-specific effector VepA) and its amino-terminal secretion signals (Akeda *et al.*, 2009), provide information for future experiments that will identify the determinants specifying effector secretion via individual T3SSs.

The T3SS2-associated chaperone identified, VocC, did not show high homology with other T3SS-associated chaperones, including the T3SS1-associated chaperone VecA, using BLAST analysis, and a few homologs (similarity > 60%) were only found in *Vibrio*, *Shewanella*, and *Photorhabdus* species equipped with T3SSs. However, the amino-terminal regions (1–100 amino acids) of the T3SS2 effectors used in this study (VopC, VopL, and VopT) did not have significant similarity with the amino termini (1–100 amino acids) of other T3SS effectors but had significant similarity with each other, as analyzed

using a new multiple sequence alignment program, MAFFT (http://www.genome.jp/tools/mafft/) (Katoh *et al.*, 2002). This result suggested that VocC and its cognate substrate of T3SS2 effectors (VopC and presumably, VopL and VopT) could be a unique combination of effectors and a chaperone among T3SSs. However, an interaction between VocC and VopL or VopT was not clearly demonstrated in this study, and other chaperones might exist for these effectors. Interestingly, VopP, which does not appear to be a cognate substrate for VocC, has a 16-amino acid gap in the sequence alignment of the first 100 amino acids compared with the other T3SS2 effectors used in the screening of this study. This may be the reason that VopP did not pull down VocC in the screening, and VopP may require other chaperones, or it could be secreted through only its possible amino-terminal secretion signal. The expression of whole T3SS2 genes encoded in Vp-PAI is regulated by VtrA and VtrB under several different conditions (Gotoh *et al.*, 2010; Kodama *et al.*, 2010), and this expression is closely correlated with secretion through T3SS2. From these results, secreted T3SS2 effectors and their cognate chaperone appeared to be expressed under the same conditions; therefore, VopP may not require a specific chaperone for its secretion. This hypothesis should be examined by further experiments.

Amino-terminal secretion signals have been proven to be important for the secretion of T3SS effectors, but there are no detectable sequence similarities among these secretion signals using traditional alignment methods, such as BLAST. However, recent computational analysis involving data integration methods of machine-learning techniques to train on sets of known T3SS effectors has revealed that the amino-terminal secretion signal of T3SS effectors could be taxonomically universal and conserved in animal and plant pathogens (Arnold *et al.*, 2009; Lower & Schneider, 2009; Samudrala *et al.*, 2009; Yang *et al.*, 2010). This finding implies that the amino-terminal secretion signal could be interchangeable between T3SS effectors originating from different bacteria. The amino-terminal secretion signal itself may interact with ATPases in any T3SSs (Sorg *et al.*, 2006) or with other T3SS components for efficient secretion. In other words, T3SS-associated chaperones alone may be the determinant for specific secretion in certain cases. Based on this hypothesis, the mechanism of the specificity of T3SS1 or 2 effector secretion should be tested by the specific interaction of their cognate chaperones (VepA and VocC) and other T3SS1 or two components, such as T3SS-associated ATPase (Akeda & Galán, 2005) or the recently identified secretion-sorting platform in *Salmonella*, SpaO-OrgA-OrgB (Lara-Tejero *et al.*, 2011), which are known to interact with T3SS effector–chaperone complexes. These experiments would clarify which molecules determine the specificity of T3SS effector secretion in *V. parahaemolyticus*.

Acknowledgements

This work was supported by Grants-in-Aid for Young Scientists and Scientific Research in Priority Areas from the Ministry of Education, Culture, Sports, Science and Technology of Japan and from the Takeda Science Foundation.

References

Akeda Y & Galán JE (2005) Chaperone release and unfolding of substrates in type III secretion. *Nature* **437**: 911–915.

Akeda Y, Okayama K, Kimura T, Dryselius R, Kodama T, Oishi K, Iida T & Honda T (2009) Identification and characterization of a type III secretion-associated chaperone in the type III secretion system 1 of *Vibrio parahaemolyticus*. *FEMS Microbiol Lett* **296**: 18–25.

Arnold R, Brandmaier S, Kleine F, Tischler P, Heinz E, Behrens S, Niinikoski A, Mewes HW, Horn M & Rattei T (2009) Sequence-based prediction of type III secreted proteins. *PLoS Pathog* **5**: e1000376.

Attree O & Attree I (2001) A second type III secretion system in *Burkholderia pseudomallei*: who is the real culprit? *Microbiology* **147**: 3197–3199.

Burdette DL, Seemann J & Orth K (2009) *Vibrio* VopQ induces PI3-kinase-independent autophagy and antagonizes phagocytosis. *Mol Microbiol* **73**: 639–649.

Coburn B, Sekirov I & Finlay BB (2007) Type III secretion systems and disease. *Clin Microbiol Rev* **20**: 535–549.

Darwin KH & Miller VL (2001) Type III secretion chaperone-dependent regulation: activation of virulence genes by SicA and InvF in *Salmonella typhimurium*. *EMBO J* **20**: 1850–1862.

Feldman MF & Cornelis GR (2003) The multitalented type III chaperones: all you can do with 15 kDa. *FEMS Microbiol Lett* **219**: 151–158.

Francis MS, Wolf-Watz H & Forsberg A (2002) Regulation of type III secretion systems. *Curr Opin Microbiol* **5**: 166–172.

Galan JE (2009) Common themes in the design and function of bacterial effectors. *Cell Host Microbe* **5**: 571–579.

Galan JE & Wolf-Watz H (2006) Protein delivery into eukaryotic cells by type III secretion machines. *Nature* **444**: 567–573.

Gotoh K, Kodama T, Hiyoshi H, Izutsu K, Park KS, Dryselius R, Akeda Y, Honda T & Iida T (2010) Bile acid-induced virulence gene expression of *Vibrio parahaemolyticus* reveals a novel therapeutic potential for bile acid sequestrants. *PLoS ONE* **5**: e13365.

Hartleib S, Prager R, Hedenstrom I, Lofdahl S & Tschape H (2003) Prevalence of the new, SPI1-like, pathogenicity island ETT2 among *Escherichia coli*. *Int J Med Microbiol* **292**: 487–493.

Hiyoshi H, Kodama T, Iida T & Honda T (2010) Contribution of *Vibrio parahaemolyticus* virulence factors to cytotoxicity,

enterotoxicity, and lethality in mice. *Infect Immun* **78**: 1772–1780.

Katoh K, Misawa K, Kuma K & Miyata T (2002) MAFFT: a novel method for rapid multiple sequence alignment based on fast Fourier transform. *Nucleic Acids Res* **30**: 3059–3066.

Knodler LA, Celli J, Hardt WD, Vallance BA, Yip C & Finlay BB (2002) *Salmonella* effectors within a single pathogenicity island are differentially expressed and translocated by separate type III secretion systems. *Mol Microbiol* **43**: 1089–1103.

Kodama T, Akeda Y, Kono G, Takahashi A, Imura K, Iida T & Honda T (2002) The EspB protein of enterohaemorrhagic *Escherichia coli* interacts directly with alpha-catenin. *Cell Microbiol* **4**: 213–222.

Kodama T, Rokuda M, Park KS, Cantarelli VV, Matsuda S, Iida T & Honda T (2007) Identification and characterization of VopT, a novel ADP-ribosyltransferase effector protein secreted via the *Vibrio parahaemolyticus* type III secretion system 2. *Cell Microbiol* **9**: 2598–2609.

Kodama T, Hiyoshi H, Gotoh K, Akeda Y, Matsuda S, Park KS, Cantarelli VV, Iida T & Honda T (2008) Identification of two translocon proteins of *Vibrio parahaemolyticus* type III secretion system 2. *Infect Immun* **76**: 4282–4289.

Kodama T, Gotoh K, Hiyoshi H, Morita M, Izutsu K, Akeda Y, Park PS, Cantarelli VV, Dryselius R, Iida T & Honda T (2010) Two regulators of *Vibrio parahaemolyticus* play important roles in enterotoxicity by controlling the expression of genes in the Vp-PAI region. *PLoS ONE* **5**: e8678.

Lara-Tejero M, Kato J, Wagner S, Liu X & Galan JE (2011) A sorting platform determines the order of protein secretion in bacterial type III systems. *Science* **331**: 1188–1191.

Lee SH & Galan JE (2004) Salmonella type III secretion-associated chaperones confer secretion-pathway specificity. *Mol Microbiol* **51**: 483–495.

Liverman AD, Cheng HC, Trosky JE, Leung DW, Yarbrough ML, Burdette DL, Rosen MK & Orth K (2007) Arp2/3-independent assembly of actin by *Vibrio* type III effector VopL. *P Natl Acad Sci USA* **104**: 17117–17122.

Lower M & Schneider G (2009) Prediction of type III secretion signals in genomes of gram-negative bacteria. *PLoS ONE* **4**: e5917.

Luo Y, Bertero MG, Frey EA *et al.* (2001) Structural and biochemical characterization of the type III secretion chaperones CesT and SigE. *Nat Struct Biol* **8**: 1031–1036.

Makino K, Oshima K, Kurokawa K *et al.* (2003) Genome sequence of *Vibrio parahaemolyticus*: a pathogenic mechanism distinct from that of *V. cholerae*. *Lancet* **361**: 743–749.

Ono T, Park KS, Ueta M, Iida T & Honda T (2006) Identification of proteins secreted via *Vibrio parahaemolyticus* type III secretion system 1. *Infect Immun* **74**: 1032–1042.

Park KS, Ono T, Rokuda M, Jang MH, Okada K, Iida T & Honda T (2004) Functional characterization of two type III secretion systems of *Vibrio parahaemolyticus*. *Infect Immun* **72**: 6659–6665.

Parsot C, Hamiaux C & Page AL (2003) The various and varying roles of specific chaperones in type III secretion systems. *Current Opin Microbiol* **6**: 7–14.

Pilonieta MC & Munson GP (2008) The chaperone IpgC copurifies with the virulence regulator MxiE. *J Bacteriol* **190**: 2249–2251.

Pineyro P, Zhou X, Orfe LH, Friel PJ, Lahmers K & Call DR (2010) Development of two animal models to study the function of *Vibrio parahaemolyticus* type III secretion systems. *Infect Immun* **78**: 4551–4559.

Samudrala R, Heffron F & McDermott JE (2009) Accurate prediction of secreted substrates and identification of a conserved putative secretion signal for type III secretion systems. *PLoS Pathog* **5**: e1000375.

Sorg JA, Blaylock B & Schneewind O (2006) Secretion signal recognition by YscN, the *Yersinia* type III secretion ATPase. *P Natl Acad Sci USA* **103**: 16490–16495.

Sory MP, Boland A, Lambermont I & Cornelis GR (1995) Identification of the YopE and YopH domains required for secretion and internalization into the cytosol of macrophages, using the cyaA gene fusion approach. *P Natl Acad Sci USA* **92**: 11998–12002.

Sugiyama T, Iida T, Izutsu K, Park KS & Honda T (2008) Precise region and the character of the pathogenicity island in clinical *Vibrio parahaemolyticus* strains. *J Bacteriol* **190**: 1835–1837.

Trosky JE, Mukherjee S, Burdette DL, Roberts M, McCarter L, Siegel RM & Orth K (2004) Inhibition of MAPK signaling pathways by VopA from *Vibrio parahaemolyticus*. *J Biol Chem* **279**: 51953–51957.

Yahr TL & Wolfgang MC (2006) Transcriptional regulation of the *Pseudomonas aeruginosa* type III secretion system. *Mol Microbiol* **62**: 631–640.

Yang Y, Zhao J, Morgan RL, Ma W & Jiang T (2010) Computational prediction of type III secreted proteins from gram-negative bacteria. *BMC Bioinformatics* **11**(suppl 1): S47.

Yarbrough ML, Li Y, Kinch LN, Grishin NV, Ball HL & Orth K (2009) AMPylation of Rho GTPases by *Vibrio* VopS disrupts effector binding and downstream signaling. *Science* **323**: 269–272.

J Infect Chemother
DOI 10.1007/s10156-011-0341-z

CASE REPORT

Recurrent bacterial meningitis by three different pathogens in an isolated asplenic child

Yoshiko Uchida · Kousaku Matsubara · Tamaki Wada · Kazunori Oishi · Tomohiro Morio · Hidetoshi Takada · Aya Iwata · Kazuo Yura · Katsunori Kamimura · Hiroyuki Nigami · Takashi Fukaya

Received: 13 July 2011 / Accepted: 25 October 2011

Abstract Isolated congenital asplenia (ICA) is a rare condition at risk for overwhelming infection. When complicated by invasive infection, the mortality remains high, at greater than 60%. We describe a girl with ICA who developed recurrent meningitis by three different pathogens. The first, meningitis by *Escherichia coli*, occurred 4 days after premature birth. The other two pathogens were serotype 6B *Streptococcus pneumoniae* and *Haemophilus influenzae* type b (Hib), at 18 and 25 months of age, respectively. The patient was successfully treated with prompt antimicrobial therapy in all episodes. Serum anti-polyribosylribitol phosphate (PRP) and anti-6B-type pneumococcal antibodies were below the levels for protective activity after natural infections. Although anti-PRP antibody was significantly increased after Hib vaccination, two (6B and 19F) of seven serotype-specific pneumococcal antibodies were not elevated to protective levels after the second 7-valent pneumococcal conjugate vaccine (PCV7). We, therefore, added a third PCV7. To our knowledge, this is the first neonatal ICA patient with invasive infection and the first case of bacterial meningitis occurring three times. Our findings indicate that monitoring of immune responses after natural infections and vaccinations, and reevaluations of vaccine schedule, are important for ICA patients to prevent subsequent invasive infections.

Keywords Isolated congenital asplenia · Bacterial meningitis · Immunological response · Recurrence · Neonate · Vaccine

Y. Uchida (✉) · K. Matsubara · T. Wada · A. Iwata · K. Yura · K. Kamimura · H. Nigami · T. Fukaya
Department of Pediatrics, Nishi-Kobe Medical Center, 5-7-1 Kojidai, Nishi-ku, Kobe 651-2273, Japan
e-mail: s00-081@nms.ac.jp

K. Oishi
Research Institute for Microbial Diseases, Osaka University, 3-1 Yamadaoka, Suita, Osaka 565-0871, Japan

T. Morio
Department of Pediatrics and Developmental Biology, Tokyo Medical and Dental University Graduate School of Medical and Dental Sciences, 1-5-45 Yushima, Bunkyo-ku, Tokyo 113-8519, Japan

H. Takada
Department of Pediatrics, Graduate School of Medical Sciences, Kyushu University, 3-1-1 Maidashi, Higashi-ku, Fukuoka 812-8582, Japan

Introduction

Congenital asplenia often occurs as part of a recognized malformation syndrome with anomalies of the heart, great vessels, and viscera [1]. The best known among these syndromes is the asplenia/polysplenia syndrome associated with visceroarterial heterotaxy, and its incidence is estimated at approximately 1/10,000 to 1/40,000 live births [2]. In contrast, isolated congenital asplenia (ICA) occurs fairly more infrequently. A recent French nationwide study indicated that the prevalence is 0.51 per million births [2]. Both conditions have an increased susceptibility to overwhelming invasive infections, carrying considerable mortality. However, the diagnosis of ICA is sometimes difficult because of the lack of other anomalies; therefore, such individuals may be unrecognized until postmortem autopsy.

Practice guidelines for the prevention of life-threatening infections in children with hyposplenia and asplenia advocate antibiotic prophylaxis and immunizations against *Streptococcus pneumoniae* and *Haemophilus influenzae* type b (Hib), the most common causative organisms for

Published online: 17 November 2011

these patients [3]. However, given that several asplenic cases of overwhelming infections that could be considered as vaccine failures have been documented [4, 5], the immunogenicity of vaccination for asplenic patients is still an important concern.

We present here a girl with ICA who developed multiple episodes of meningitis caused by three different pathogens, namely, *Escherichia coli*, *S. pneumoniae* (serotype 6B), and Hib. She was successfully treated with prompt initiation of antibiotics in all episodes. We also present the details of immune responses to natural infections by Hib and serotype 6B *S. pneumoniae* and those to immunizations of Hib conjugate vaccine and 7-valent pneumococcal conjugate vaccine (PCV7).

Case report

A 4-day-old girl, who was born of nonconsanguineous parents as their first child, weighing 1,742 g at the 34th week of gestation, presented with repetitive apnea during admission because of prematurity. Physical examination showed that heart rate was 135/min and body temperature was 37.2°C. Laboratory data showed WBC of 5.8×10^9/l with 28.5% neutrophils, C-reactive protein (CRP) of 4.3 mg/dl, and blood glucose of 95 mg/dl. Cerebrospinal fluid (CSF) examination showed 3,947 cells/μl with 96% polymorphonuclear cells, 197 mg/dl protein, and 44 mg/dl glucose. Two days later, isolates from the CSF and blood were identified as *E. coli* OX:K1:H–, and the same bacterium was also subsequently isolated from the stool of her asymptomatic mother. The patient was diagnosed as having early-onset *E. coli* meningitis that was vertically transmitted. We treated the patient with cefotaxime (CTX) for 21 days. Auditory brainstem response examination at 28 days of age revealed profound hearing impairment at the right ear. The patient was discharged at 38 days of age. Genetic analysis [6, 7] showed that the strain harbored virulence factor genes such as *iroN*, *papG3*, *afa*, and *kps*, but not *cnf1*, *sfa*, or *ibeA*.

At 18 months old, the patient was rehospitalized because of a 6-h history of fever and generalized tonic-clonic convulsion lasting 3 min. On admission, 30 min after the convulsion, heart rate was 170/min and body temperature was 39.4°C. Her consciousness had become clear. Laboratory findings showed WBC of 21.7×10^9/l and CRP of 6.0 mg/dl. CSF examination showed no pleocytosis, with normal concentrations of protein (10 mg/dl) and glucose (85 mg/dl). Treatment with intravenous CTX was empirically initiated under the tentative diagnosis of occult bacteremia. The day after admission, serotype 6B *S. pneumoniae* was isolated from the blood but not from the CSF. Resistance to penicillin was established by microbiological [minimum inhibitory concentration (MIC), 2 μg/ml] and genotypic (mutations in *pbp1a*, *pbp2X*, and *pbp2b* [8]) analyses, and CTX was substituted with panipenem–betamipron. On day 3, prolonged fever and frequent vomiting led us to perform a second CSF examination, showing 14,500 cells/μl, protein of 58 mg/dl, and glucose of 63 mg/dl. The CSF was positive for *S. pneumoniae* antigen test (Binax NOW *S. pneumoniae*; Binax), but yielded no organisms in culture. The blood WBC and CRP were elevated to 21.7×10^9/l and 22.1 mg/dl, respectively. We diagnosed her disease as pneumococcal meningitis following bacteremia and increased the doses of panipenem–betamipron with good clinical response. She received antimicrobial therapy for 14 days and was discharged without any additional sequelae.

At 25 months of ages, the patient was referred to the emergency department in another hospital with a 2-h history of fever, vomiting, and tonic–clonic convulsion of 2-min duration. At arrival, heart rate was 180/min and body temperature was 39.4°C. Her consciousness soon became clear. Laboratory examination showed WBC of 3.5×10^9/l and CRP of 0.6 mg/dl. After blood culture was obtained, the patient received intravenous sulbactam/ABPC. On day 3, the blood culture yielded β-lactamase-non-producing ABPC-resistant (BLNAR) Hib, and the laboratory examinations showed marked deterioration: WBC of 26.6×10^9/l and CRP of 21.5 mg/dl. CSF examination showed 4,992 cells/μl, 164 mg/dl protein, and 34 mg/dl glucose with positive culture for Hib. Thus, the diagnosis of a third bacterial meningitis was made. The patient thereafter received intravenous meropenem for 14 days and was discharged on day 16 after onset without any additional sequelae. Molecular analysis of the strain identified three amino acid substitutions: His-517, Thr-385, and Ile-377, in *ftsI* [9]. This substitution pattern was classified as subgroup III BLNAR by a recent nationwide study of childhood meningitis in Japan [9].

The multiple episodes of meningitis prompted us to evaluate immunological functions. The results after the second episode of meningitis showed that serum levels of IgG (639 mg/dl), IgA (65 mg/dl), IgM (97 mg/dl), IgG_2 (80 mg/dl), C3 (140 mg/dl), C4 (24 mg/dl), and CH50 (36.1 U/ml) were within normal limits. T/B-cell subsets (65/28%), CD3/CD4/CD8 lymphocyte subsets (61%/44%/14%), natural killer cell activity (25%), neutrophil phagocytic activity using fluorescence bead test by flow cytometry (70.0%), and neutrophil bacteriocidal activity (93.4%) were also normal. Computed tomography (CT) of the skull and inner ears did not show any deformity or defects. To screen interleukin-1 receptor-associated kinase 4 deficiency and myeloid differentiation primary response protein 88 deficiency, we performed flow cytometric analysis [10], resulting in normal intracellular tumor necrosis factor-α

production of monocytes after lipopolysaccharide stimulation. After the third meningitis, ultrasonography and CT of the abdomen finally revealed asplenia without visceroarterial anomalies. Howell–Jolly body-containing RBCs were exceedingly rarely found (<0.1% of RBCs) in peripheral blood. Ultrasonographic examinations of her parents detected normal size and normal position of the spleen.

Since the diagnosis of ICA at 26 months of age, chemoprophylaxis with amoxicillin of 20 mg/kg/day was introduced as well as vaccinations of Hib vaccine and PCV7. Subsequent to the introduction of these strategies, the patient has not suffered from any invasive infections for more than 2 years. At 36 months of age, we assessed her neurodevelopmental status using the New Edition of the Kyoto Scale of Psychological Development, indicating a normal developmental quotient of 88 (normal range, >80).

We evaluated immune responses to natural infections with Hib and serotype 6B pneumococcus and those to immunizations of Hib vaccine and PCV7 (Table 1). Despite natural infections, serum anti-polyribosylribitol phosphate (PRP) (0.60 μg/ml) and anti-serotype 6B (0.191 μg/ml) antibodies were below the levels of long-term protective activity (1.0 μg/ml [11] and 0.34 μg/ml [12, 13], respectively) 4 and 6 months after each infection, respectively. At 1 month after administration of the second Hib and PCV7 vaccination, anti-PRP antibody was significantly elevated to 3.15 μg/ml, but two (6B and 19F) of seven serotype-specific pneumococcal antibodies were still below the protection levels. We therefore added a third PCV7. Because antibodies to pneumococcal capsular polysaccharide protect the host by opsonizing pneumococci for phagocytosis, we concomitantly performed the opsonophagocytic killing assay (OPA) [14] after the third PCV7. Table 1 shows significantly high OPA titers against types 6B and 19F were observed, findings inconsistent with the low anti-6B and anti-19F IgG antibody levels. OPA titers against five other types were also elevated to the levels for protection (>8) [12, 13].

Discussion

We report a girl with non-familial ICA with recurrent bacterial meningitis. ICA is a rare anomaly. Mahlaoui et al. [2] recently documented 20 ICA cases in France and reviewed the literature. In addition to the 65 cases in their report and references therein [2], we found reports of 5 other ICA patients [5, 15] in the literature between January 1960 and April 2011 using the Medline database. Thus, we can here review 70 ICA cases in total. Compared with these patients [2, 5, 15], our case is informative and interesting in several respects.

First are the multiple episodes of meningitis caused by three different pathogens. Of the previous 70 cases, 48 (69%) experienced invasive bacterial infection at least once. Of these 48 patients, only 8 had multiple episodes of invasive bacterial infections, two times in 5 cases and three times in 3 cases (Table 2) [2, 16–20]. Our patient is the first described for whom all three episodes were bacterial meningitis. To better understand the underlying pathogenesis, we characterized the causative pathogens by molecular analysis. Penicillin-resistant serotype 6B pneumococcus and BLNAR Hib subgroup III were among the most prevalent strains causing childhood meningitis in Japan [8, 9]. In contrast, *E. coli* is extremely rare among ICA patients, and we are aware of only one such case, which resulted in death at 4 months of age [21]. *E. coli* in our case possessed capsular antigen K1 and the siderophore receptor gene, *iroN*, which contribute to the bacteremic step in *E. coli* neonatal meningitis [7, 22]. Because the same strain was isolated from the stool of her asymptomatic mother, we confirmed the route of contagion. Besides asplenia, prematurity of the host and high pathogenic factors of the *E. coli* strain might have contributed to this infection.

Second is the good prognosis, despite our patient developing meningitis three times, one of which occurred 4 days after premature birth. Our neonatal case is the youngest at the first invasive infection among the previously reported ICA patients. There have been only 3 ICA patients

Table 1 Serum serotype-specific IgG antibody concentrations and opsonophagocytic killing assay titer before and after 7-valent pneumococcal conjugate vaccine

Serotype	4		6B		9V		14		18C		19F		23F	
	IgG conc.	OPA	IgG conc.	OPA	IgG conc.	OPA	IgG conc.	OPA	IgG conc.	OPA	IgG conc.	OPA	IgG conc.	OPA
Before PCV7 (6 months after natural infection)	0.132	NA	0.191	NA	0.062	NA	0.366	NA	4.229	NA	0.295	NA	0.14	NA
1 month after 2-dose PCV7	2.809	NA	0.263	NA	4.040	NA	6.767	NA	3.949	NA	0.356	NA	0.233	NA
1 month after 3-dose PCV7	1.37	536	0.137	557	1.199	326	5.075	2367	1.89	210	0.295	192	0.471	769

PCV7 7-valent pneumococcal conjugate vaccine, *IgG conc.* anti-serotype-specific IgG antibody concentration (μg/ml), *OPA* opsonophagocytic killing assay (titer), *NA* not assessed (under treatment with antimicrobial agents)

Table 2 Isolated congenital asplenia patients with multiple episodes of invasive bacterial infections

Patient number	Gender	Infectious episodes	Age at onset	Type of infection	Organisms	Outcome	Reference
1	F	1	6 months	Meningitis	*Streptococcus pneumoniae*	Survived	[2]
		2	11 months	Meningitis, purpura fulminans	*S. pneumoniae*	Died	
2	M	1	10 months	Meningitis	*S. pneumoniae*	Survived	[2]
		2	11 months	Purpura fulminans	*S. pneumoniae*	Survived	
		3	1 year 7 months	Purpura fulminans	*S. pneumoniae*	Survived	
3	M	1	1 year 9 months	Meningitis	*S. pneumoniae*	Survived	[16]
		2	2 years 3 months	Meningitis	*S. pneumoniae*	Survived	
4	M	1	1 year 2 months	Meningitis	*S. pneumoniae*	Survived	[17]
		2	15 years	Meningitis	Not available	Died	
5	M	1	1 year	Meningitis	*S. pneumoniae*	Survived	[18]
		2	1 year	Meningitis	*S. pneumoniae*	Survived	
		3	1 year	Osteomyelitis	Culture negative	Survived	
6	F	1	6 months	Meningitis	*S. pneumoniae*	Survived	[19]
		2	2 years 6 months	Sepsis	Not available	Died	
7	F	1	1 year 6 months	Arthritis	*S. pneumoniae*	Survived	[19]
		2	1 year 9 months	Arthritis	*Haemophilus influenzae* type b	Survived	
		3	10 years	Sepsis	*S. pneumoniae*	Died	
8	M	1	5 years	Sepsis	*S. pneumoniae*	Survived	[20]
		2	9 years	Meningitis	*S. pneumoniae*	Died	
9	F	1	0 month (4 days)	Meningitis	*Escherichia coli*	Survived	Present case
		2	1 year 6 months	Meningitis	*S. pneumoniae*	Survived	
		3	2 years 1 month	Meningitis	*H. influenzae* type b	Survived	

who had overt infections under 3 months of age, which include 1 fatal case [21] and 2 with major sequelae (central nervous system deficit [23] or loss of foot and fingers [24]). Of the 45 childhood and adult patients with invasive infections whose outcomes were known, 29 (64%) died and 3 (7%) had serious sequelae [2, 5, 23, 24]. In contrast, our patient showed normal neurological development under non-serious sequelae of unilateral hearing loss. Such favorable outcome may be attributable to the early recognition and hospitalization. Fortunately, the first episode developed during the period of hospitalization under close monitoring because of prematurity. In addition, at both second and third infectious episodes, she could receive immediate antimicrobial treatment.

Finally, we meticulously investigated the immunological responses to natural infections with *S. pneumoniae* and Hib and those to vaccinations. Of the 70 cases we can review [2, 5, 15], there has been no report addressing this issue. The spleen is a pivotal organ for the phagocytosis of encapsulated bacteria and for the production of immunoglobulins against these pathogens [3]. Even after natural invasive infections of Hib and serotype 6B pneumococcus, serum antibody levels were not elevated to the levels of long-term protection against the pathogens, which may reflect the immunocompromised status of asplenia. This concept is supported by findings from Mikoluc et al. [25] that the congenital asplenic patients had significantly lower concentrations of serum anti-pneumococcal antibodies and reduced responses to PCV7, especially to serotypes 6B and 23F. Similar findings were also observed in adult asplenic patients with overwhelming infection caused by *S. pneumoniae*, representing vaccine failures [4, 5]. Serum antibody concentrations against 6B and 19F in our patient were significantly lower than those against five other serotypes. In contrast, when we evaluated OPA titers after the third PCV7 vaccination, they were at sufficient levels for protection against all serotypes including types 6B and 19F. OPA might be a more important indicator for protection against *S. pneumoniae* [13].

In conclusion, we described a girl with a rare case of ICA, who presented with recurrent meningitis caused by three different pathogens, and was successfully treated without severe sequelae. Exact determination of serum antibody concentrations of encapsulated bacteria and reevaluation of vaccine schedules should be important to protect against relevant infections in ICA patients.

References

1. Ivemark BI. Implications of agenesis of the spleen on the pathogenesis of conotruncus anomalies in childhood: an analysis of the heart malformations in the asplenia agenesis syndrome, with fourteen new cases. Acta Paediatr Suppl. 1955;44(suppl 104) :7–110.
2. Mahlaoui N, Minard-Colin V, Picard C, Bolze A, Ku CL, Tournilhac O, et al. Isolated congenital asplenia: a French nationwide retrospective survey of 20 cases. J Pediatr. 2011;158: 106–12.
3. Price VE, Blanchette VS, Ford-Jones EL. The prevention and management of infections in children with asplenia or hyposplenia. Infect Dis Clin N Am. 2007;21:697–710.
4. Waghorn DJ. Overwhelming infection in asplenic patients: current best practice preventive measures are not followed. J Clin Pathol. 2001;54:214–8.
5. Vincentelli C, Molina EG, Robinson MJ. Fatal pneumococcal Waterhouse-Friderichsen syndrome in a vaccinated adult with congenital asplenia. Am J Emerg Med 2009;27:751.e3–751.e5.
6. Johnson JR, Stell AL. Extended virulence genotypes of *Escherichia coli* strains from patients with urosepsis in relation to phylogeny and host compromise. J Infect Dis. 2000;181:261–72.
7. Bonacorsi S, Clermont O, Houdouin V, Cordevant C, Brahimi N, Marecat A, et al. Molecular analysis and experimental virulence of French and North American *Escherichia coli* neonatal meningitis isolates: identification of a new virulent clone. J Infect Dis. 2003;187:1895–906.
8. Ubukata K, Chiba N, Hasegawa K, Kobayashi R, Iwata S, Sunakawa K. Antibiotic susceptibility in relation to penicillin-binding protein genes and serotype distribution of *Streptococcus pneumoniae* strains responsible for meningitis in Japan, 1999 to 2002. Antimicrob Agents Chemother. 2004;48:1488–94.
9. Hasegawa K, Kobayashi R, Takada E, Ono A, Chiba N, Morozumi M, et al. Nationwide Surveillance for Bacterial Meningitis. High prevalence of type b β-lactamase-non-producing ampicillin-resistant *Haemophilus influenzae* in meningitis: the situation in Japan where Hib vaccine has not been introduced. J Antimicrob Chemother. 2006;57:1077–82.
10. Takada H, Yoshikawa H, Imaizumi M, Kitamura T, Takeyama J, Kumaki S, et al. Delayed separation of the umbilical cord in two siblings with interleukin-1 receptor-associated kinase 4 deficiency: rapid screening by flow cytometer. J Pediatr. 2006;148: 546–8.
11. Kelly DF, Moxon ER, Yu LM, Pollard AJ. Anti-polyribosylribitol phosphate antibody concentrations and avidities in children since the start of *Haemophilus influenzae* type b immunization of infants in the United Kingdom. Clin Vaccine Immunol. 2009;16:246–52.
12. World Health Organization. Recommendations for the production and control of pneumococcal conjugate vaccines. WHO Tech Rep Ser. 2005;927(Annex 2):64–98.
13. Feavers I, Knezevic I, Powell M, Griffiths E. WHO consultation on serological criteria for evaluation and licensing of new pneumococcal vaccines. Challenges in the evaluation and licensing of new pneumococcal vaccines, 7–8 July 2008, Ottawa, Canada. Vaccine. 2009;27:3681–8.
14. Burton RL, Nahm MH. Development and validation of a fourfold multiplexed opsonization assay (MOPA4) for pneumococcal antibodies. Clin Vaccine Immunol. 2006;13:1004–9.
15. Hummler HD, Pohlandt F, Essig A. Fulminant pneumococcal sepsis in a 13 months old child with congenital asplenia. Klin Pädiatr. 2005;217:274–5.
16. Kevy SV, Tefft M, Vawter GF, Rosen FS. Hereditary splenic hypoplasia. Pediatrics. 1968;42:752–7.
17. Gopal V, Bisno AL. Fulminant pneumococcal infections in 'normal' asplenic hosts. Arch Intern Med. 1977;137:1526–30.
18. Gill DG, Kara M. Septicaemia and adrenal haemorrhage in congenital asplenia. Arch Dis Child. 1991;66:1366.
19. Halbertsma FJJ, Neeleman C, Weemaes CM, van Deuren M. The absent and vanishing spleen: congenital asplenia and hyposplenism—two case reports. Acta Paediatr. 2005;94:369–71.
20. Araújo AR, Maciel I, Lima L, Chacim I, Barbot J. Congenital asplenia and severe visceral toxocariasis. Pediatr Infect Dis J. 2008;27:478.
21. Waldman JD, Rosenthal A, Smith AL, Shurin S, Nadas AS. Sepsis and congenital asplenia. J Pediatr. 1977;90:555–9.
22. Bonacorsi S, Bingen E. Molecular epidemiology of *Escherichia coli* causing neonatal meningitis. Int J Med Microbiol. 2005;295:373–81.
23. Honigman R, Lanzkowsky P. Isolated congenital asplenia: an occult case of overwhelming sepsis. Am J Dis Child. 1979;133:552–3.
24. Gillis J, Harvey J, Isaacs D, Freelander M, Wyeth B. Familial asplenia. Arch Dis Child. 1992;67:665–6.
25. Mikoluc B, Kayhty H, Bernatowska E, Motkowski R. Immune response to the 7-valent pneumococcal conjugate vaccine in 30 asplenic children. Eur J Microbiol Infect Dis. 2008;27:923–8.

Bedside Teaching

わが国の高齢者に対する肺炎球菌ワクチンの定期接種化は必要か？*

川上　健司[1]　赤沢　学[2]　大石　和徳[3]

はじめに

2010年度に入り，厚生労働省は今後の予防接種法改正を目指して，成人用23価ポリサッカライド肺炎球菌ワクチン(polysaccharide pneumococcal vaccine；PPV)を含む9つのワクチンに係るファクトシートをまとめた．その間に，小児ワクチンであるHPVワクチン，Hibワクチン，7価肺炎球菌結合型ワクチンの公費助成の方針を決定した．このようなわが国のワクチン行政の変革のなか，PPVの肺炎発症予防に関するエビデンスとその医療経済学的効果の重要性が注目されている．

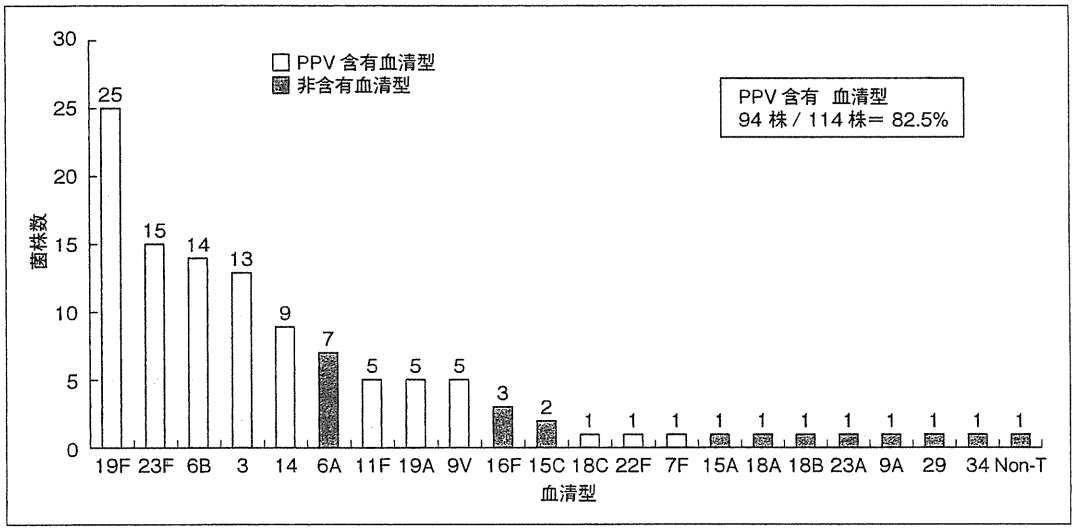

図1　わが国の市中肺炎を起こした肺炎球菌の血清型を23価肺炎球菌ワクチンはどのくらいカバーするのか？(文献[1]より引用)

* Is a Universal Vaccination of Pneumococcal Vaccine Required for the Elderly in Japan?

[1] 国立病院機構長崎川棚医療センター呼吸器内科(〒859-3615 長崎県東彼杵郡川棚町下組郷2005-1)　Kenji Kawakami：Department of Respiratory Medicine, National Hospital Organization Nagasaki Kawatana Hospital
[2] 明治薬科大学公衆衛生・疫学　Manabu Akazawa：Department of Public Health and Epidemiology, Meiji Pharmaceutical University
[3] 大阪大学微生物病研究所感染症国際研究センター　Kazunori Oishi：Research Institute for Microbial Disease, Osaka University

0452-3458/11/¥500/論文/JCOPY